SAND2015-10173C

Exceptional service in the national interest

Sandia National Laboratories

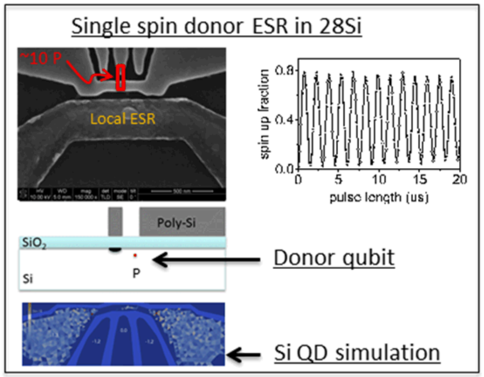

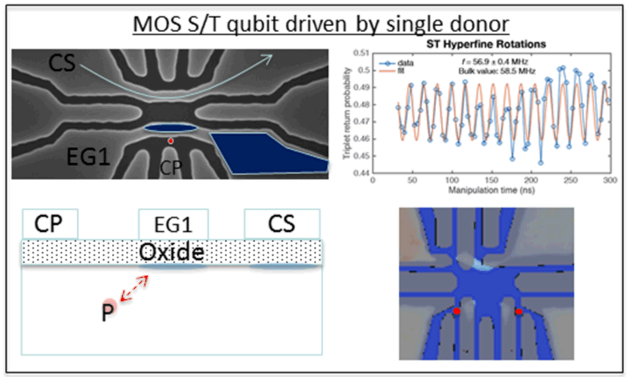

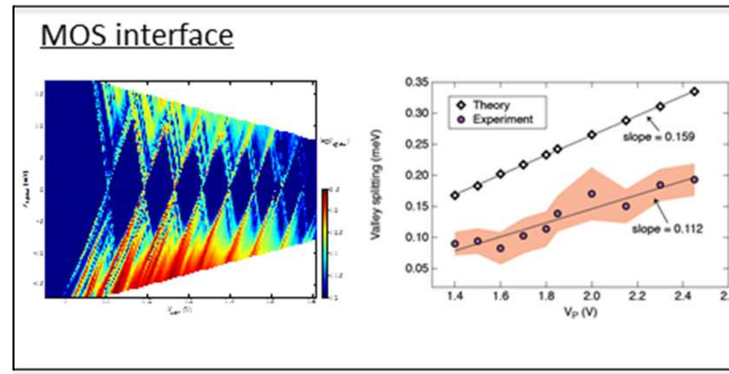

Materials and fabrication of Si qubits

Malcolm Carroll & **QIST team**

Sandia National Labs, Albuquerque, NM 87185

August 21, 2015

Sandia National Laboratories is a multi-program laboratory managed and operated by Sandia Corporation, a wholly owned subsidiary of Lockheed Martin Corporation, for the U.S. Department of Energy's National Nuclear Security Administration under contract DE-AC04-94AL85000.

Outline

- Motivations
- MOS single donor ESR qubits (natural & ^{28}Si)
- Two qubit nanostructures
  - Latch read-out for S/T qubits
  - Donor hyperfine driven S/T qubit
    - Coherent donor spin coupling to surface QD
  - New poly Si QD-D design
  - Advanced single donor fabrication (STM – single ion implant)
- Summary

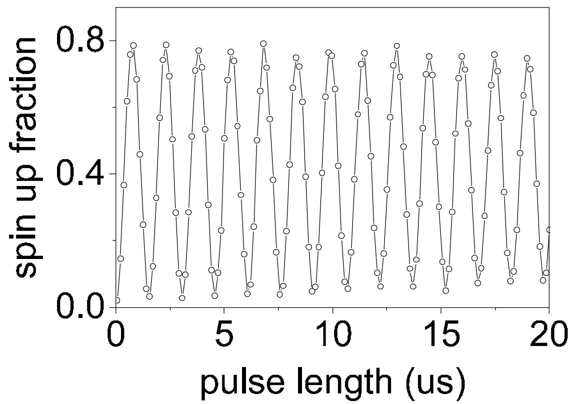

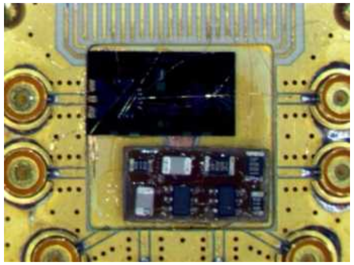

Sandia National Laboratories

Outline

- Motivations
- MOS single donor ESR qubits (natural & ^{28}Si)
- Two qubit nanostructures
  - Donor hyperfine driven S/T qubit
    - Coherent donor spin coupling to surface QD
  - New poly Si QD-D design
  - Advanced single donor fabrication (STM – single ion implant)
- Summary

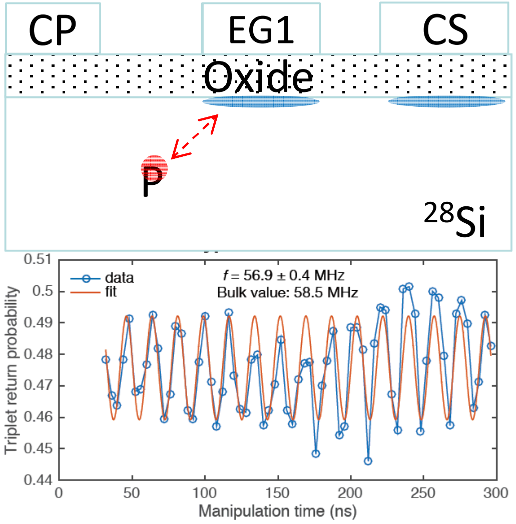

Outline

- Motivations
- MOS single donor ESR qubits (natural & ^{28}Si)

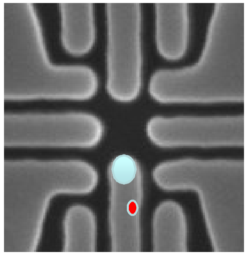

- Two qubit nanostructures
  - Donor hyperfine driven S/T qubit
    - Coherent donor spin coupling to surface QD
  - New poly Si QD & QD-D design
  - Advanced single donor fabrication (STM – single ion implant)

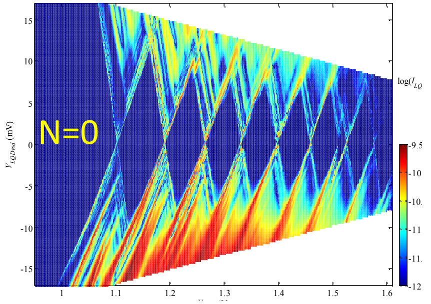

- Summary

Sandia National Laboratories

Outline

- Motivations
- MOS single donor ESR qubits (natural & ^{28}Si)
- Two qubit nanostructures
  - Latch read-out for S/T qubits
  - Donor hyperfine driven S/T qubit
    - Coherent donor spin coupling to surface QD
  - New poly Si QD-D design
  - Advanced single donor fabrication (STM – single ion implant)
- Summary

Offsets in counted implanted devices (~50% yield)

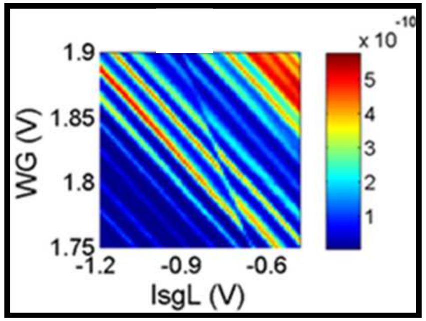

Motivation

- Some general motivations for QC
  - End of Moore's law
  - Si for QC because of potential for semiconducting "magnetic-vacuum" & Si industry platform

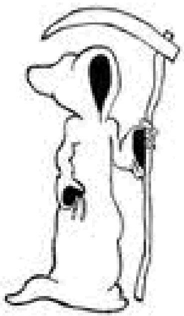

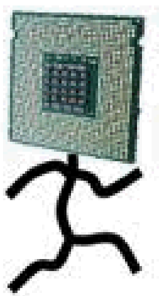

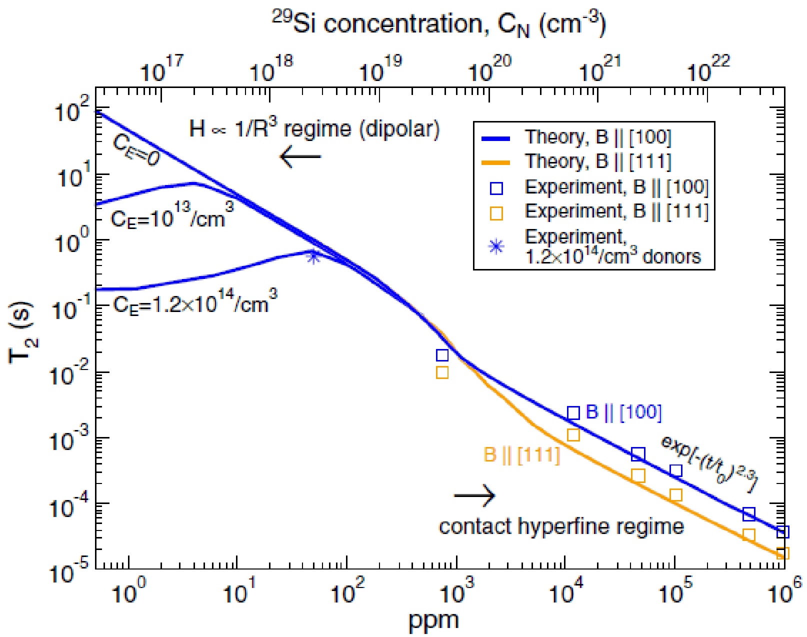

Witzel et al., PRL 105, 187602 (2010) & PRB 86 035452 (2012)

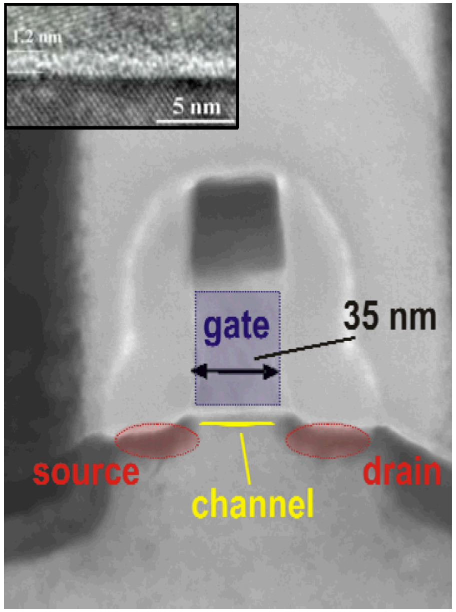

Nanostructure fabrication at Sandia National Labs

Front-end in silicon fab

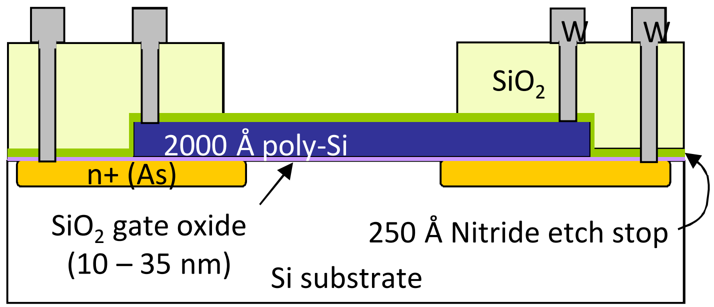

Back-end nanolithography

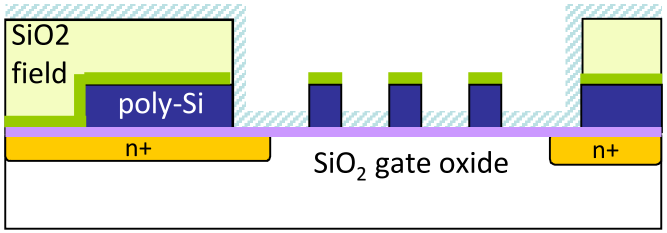

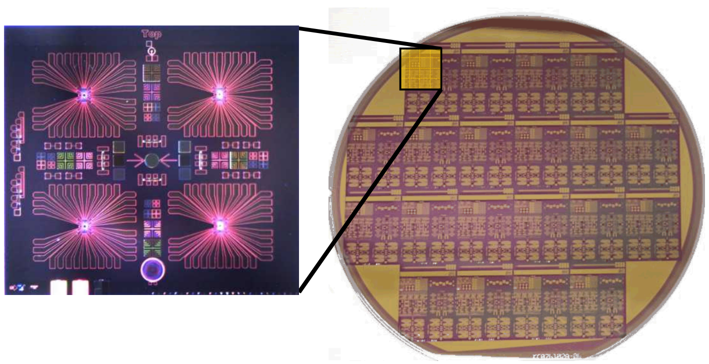

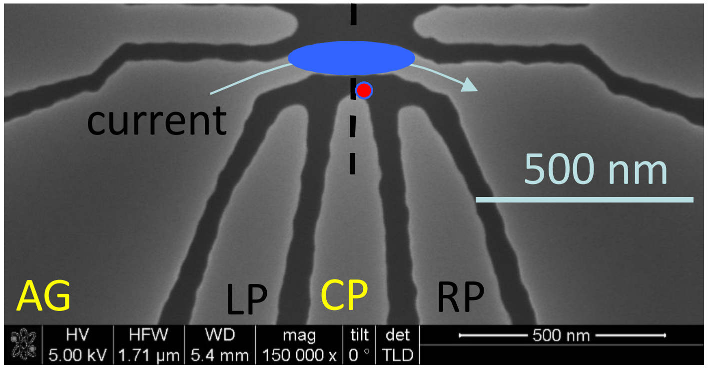

Goal: Use Poly-Si etched structures to produce donor-based qubits

Rationale:

- Self aligned implant
- Foundry like processing
- Potential long term benefits for charge stability

Nordberg et al., PRB 80 115331 (2009)

Tracy et al., APL 103 143115 (2013)

Gate wire with implant – QD coupling to donor

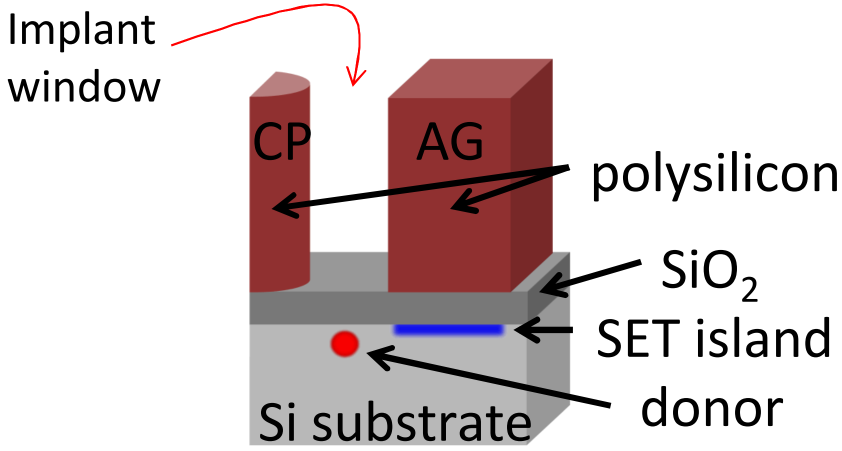

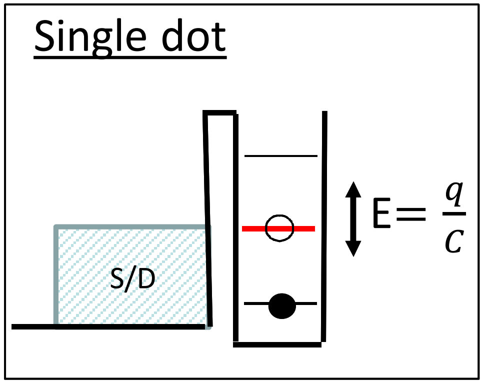

- Poly-Si gated nanostructures
- Use Poly-Si for self-alignment of donors
- Donor qubit readout through quantum dot
- Quantum dot senses the spin dependent ionization of the donor

Gate wire with implant – QD coupling to donor

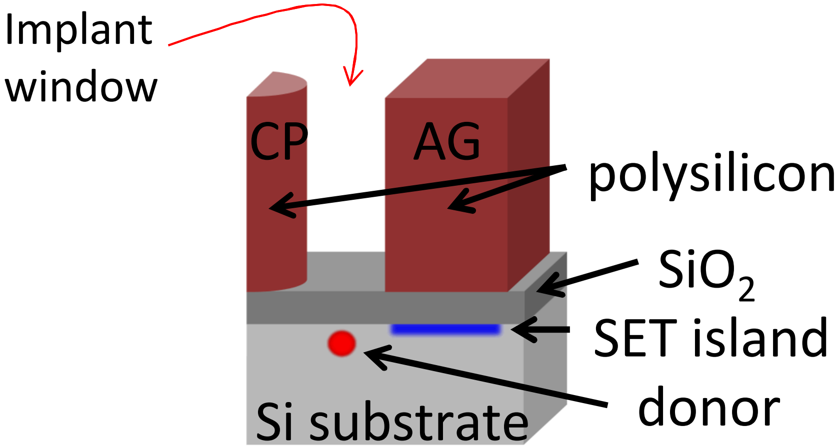

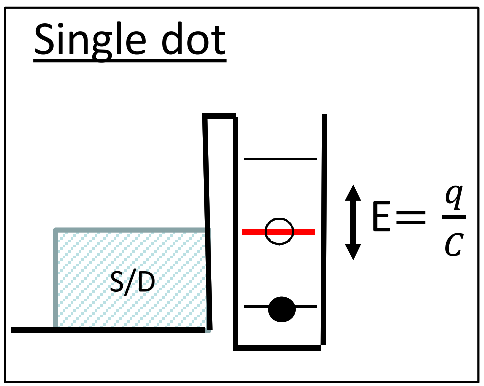

SET offsets (detection of ionization)

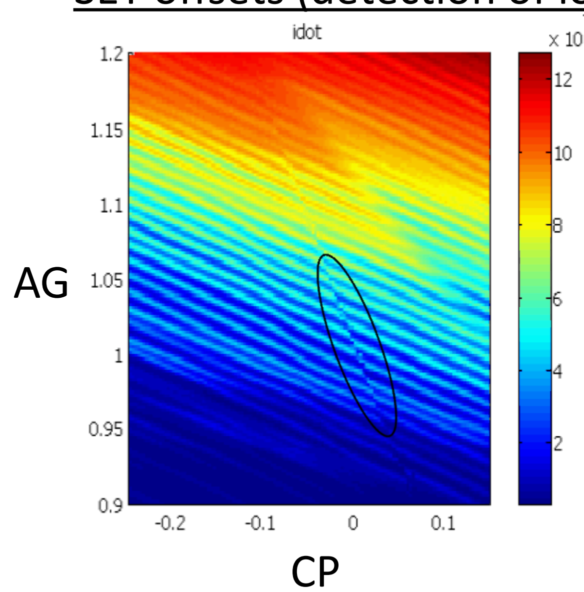

Spin dependent ionization

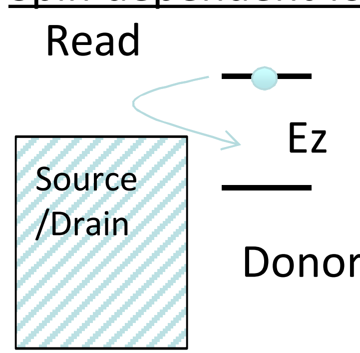

- Poly-Si gated nanostructures
- Use Poly-Si for self-alignment of donors
- Donor qubit readout through quantum dot
- Quantum dot senses the spin dependent ionization of the donor

Morello et al., Nature 2010
Tracy et al., APL 2013

Single donor qubits & dephasing metrics

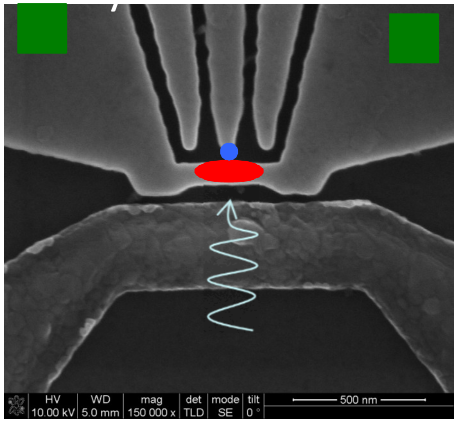

Ohmics

Donor

Quantum Dot

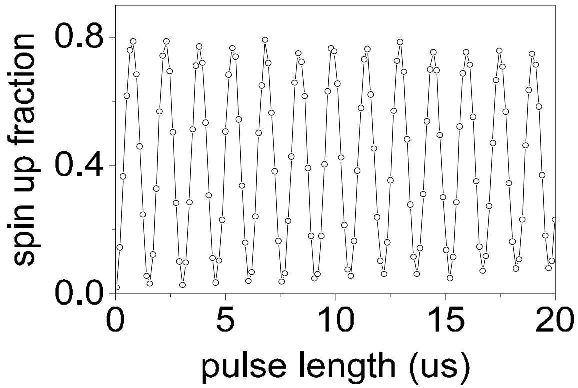

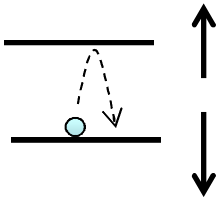

^{28}Si epilayer

- 2.5 μm thick
- 500 ppm ^{29}Si (ToF SIMS)

Nominally identical processing

- Coarse metrics of material quality with respect to spin "vacuum" are T2 & T2*
- Roughly, this is a measure of inhomogeneous local B-field from dipoles (T2*) & how rapidly that field is changing (T2)
- This case: ESR: T2 = 0.31 ms, T2* = 10-20 μs

Tracy et al. (in preparation)

Read-out circuit (AM HEMT)

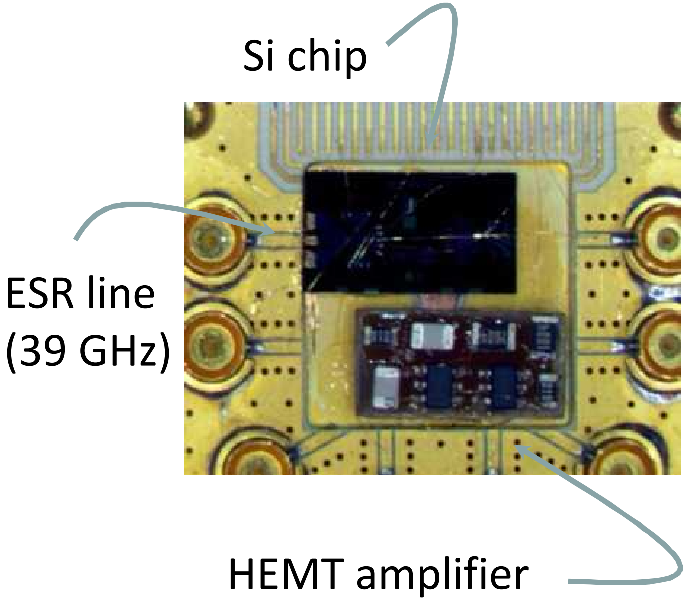

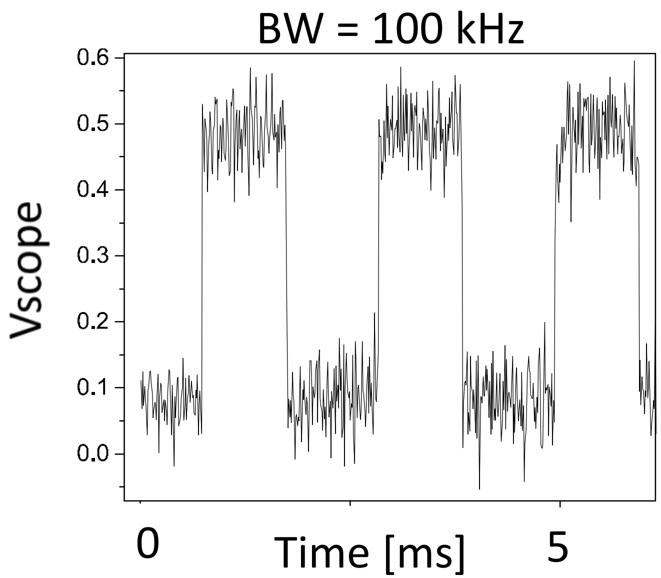

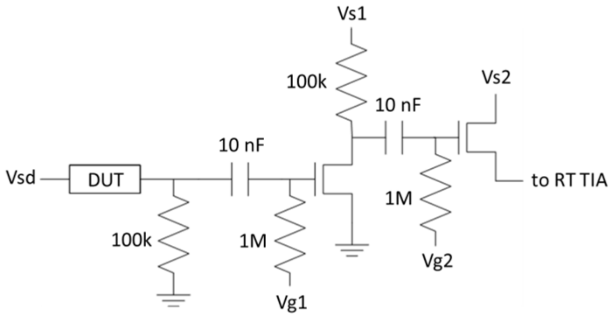

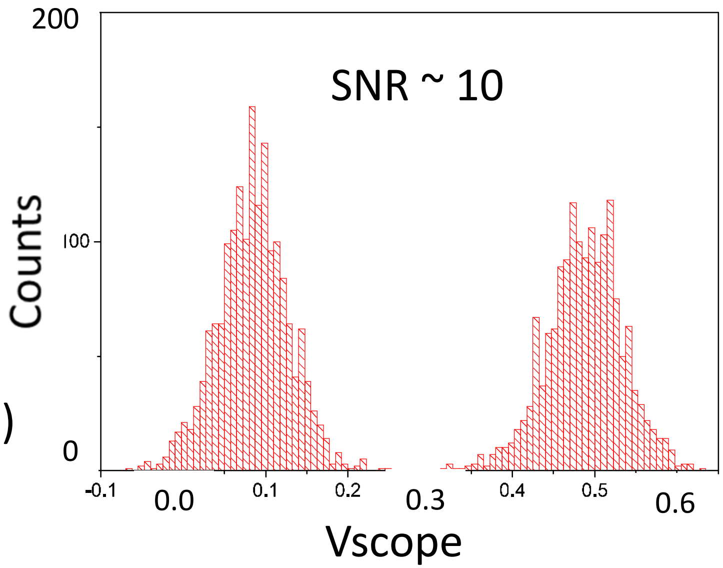

- Dry fridge noise a real nuisance
- Cryo-preamplification & AM technique (300 kHz)
- Good visibility w/ ~1% threshold overlap
- $T_{electron}$ ~ 200 mK

Poster: L. Tracy

HBT alternative?

Poster: T. England

- HBT offers better gain vs. current level in device
- Team considered "DC" solution w/HBT first
  - HBT is biased directly with SET current

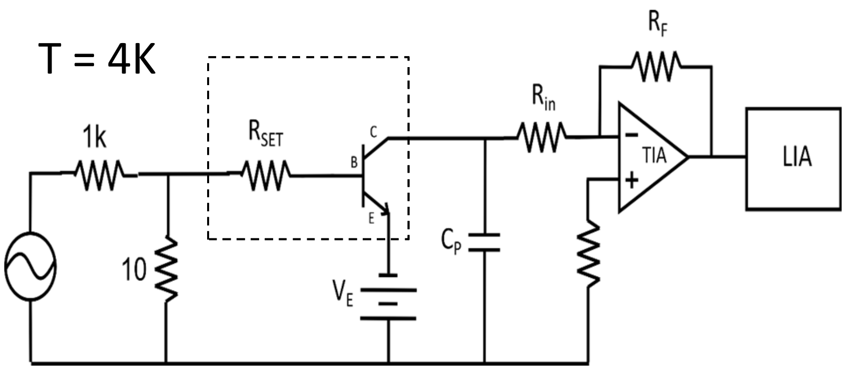

RTS with different RT pre-amplifier BWs

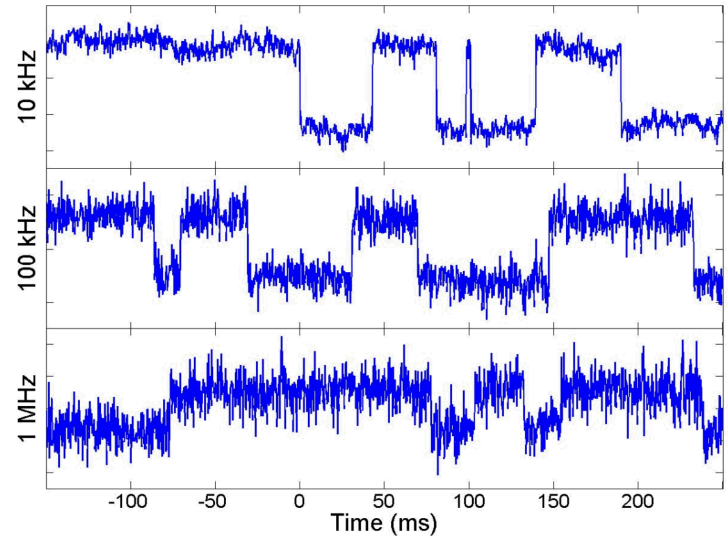

- Bandwidth is extended using HBT
- S/N appears to be improved
- Estimated max. power: ~5 uW
- *Fine print: HBT response is non-linear & V_{sd} floats*

HBT (above) compared to no-HBT (from f response)

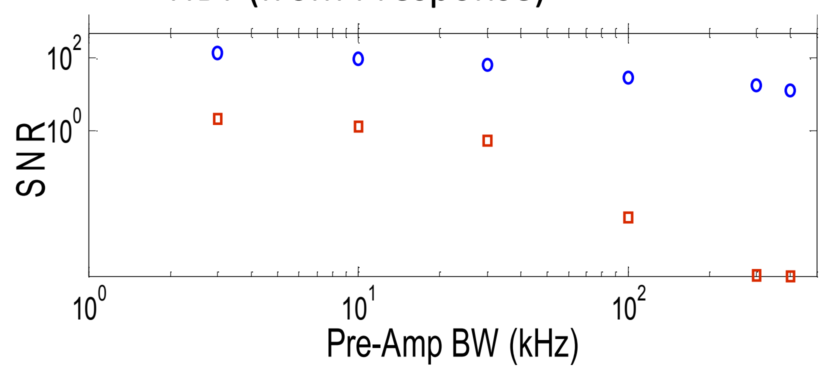

- Good result. Team is now looking to improve and is considering an AC coupling scheme to compare HEMT to HBT. Jury is still out. See poster

Curry, APL 106 202505 (2015)

Rabi oscillations

10 kHz BW

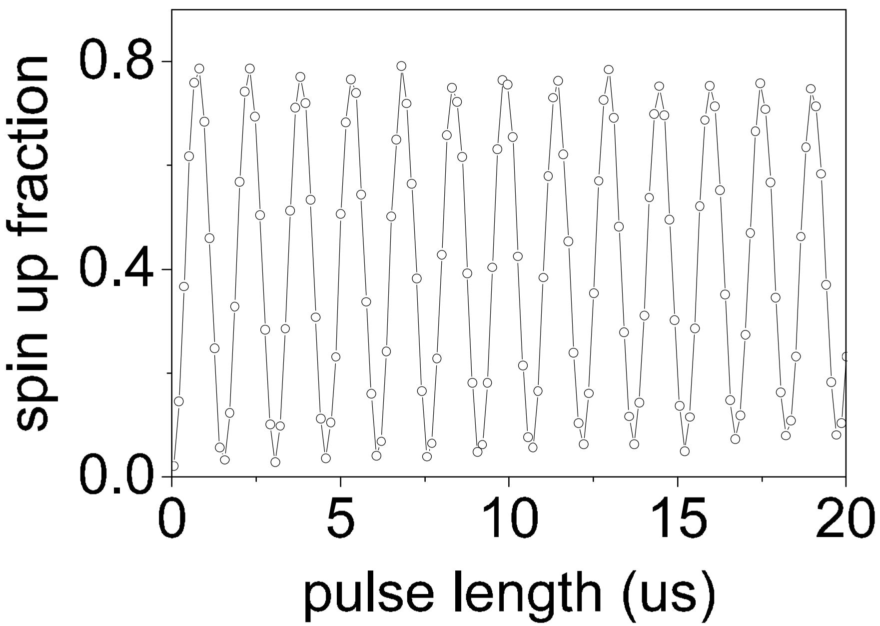

96% visibility w/100 kHz BW

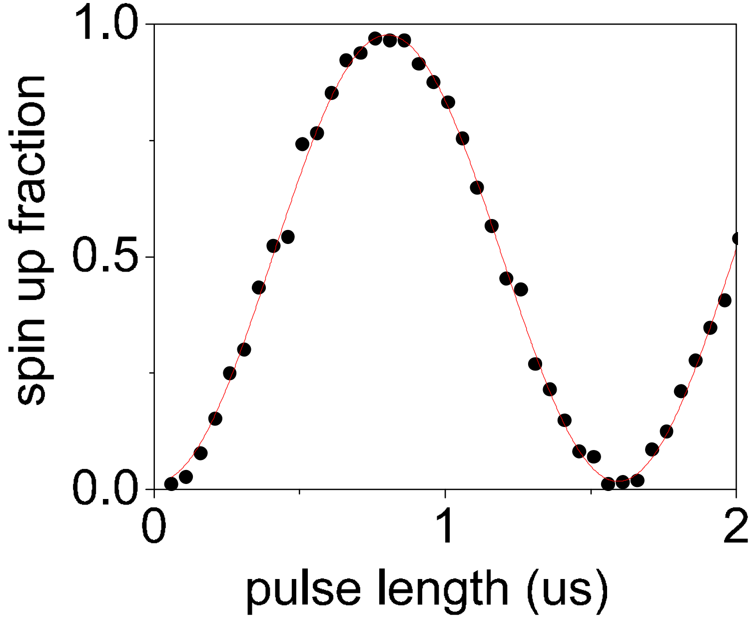

Long lived Rabi oscillations

Visibility reduced because preamplifier BW was not optimized (BW ~ 10 kHz)
For example, fast spin-up tunneling events can be missed.

Poster: L. Tracy

Single donor qubits & dephasing metrics

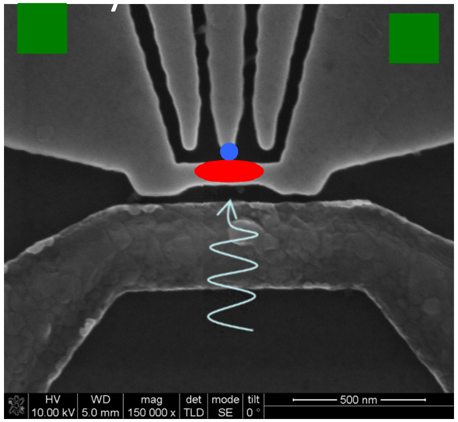

Ohmics

Donor

Quantum Dot

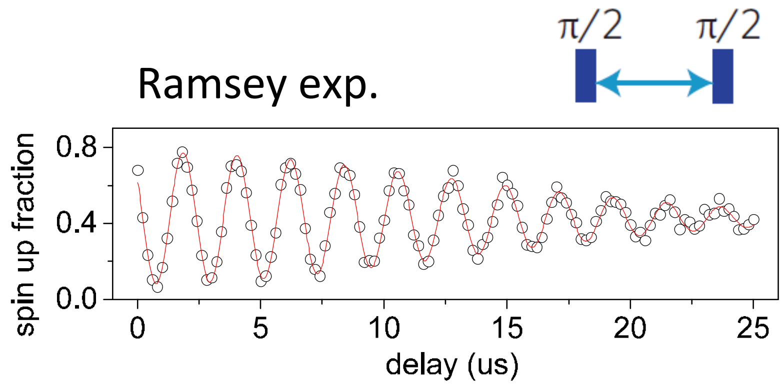

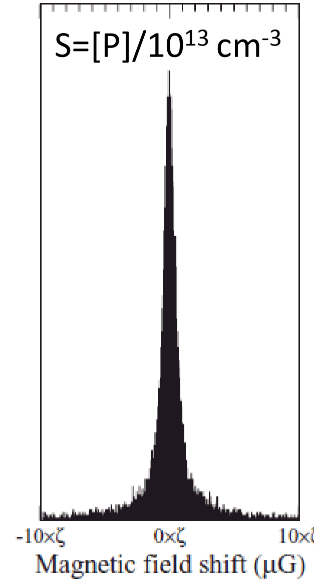

Witzel et al., PRB 2012

^{28}Si epilayer

- 2.5 μm thick
- 500 ppm ^{29}Si (ToF SIMS)

Nominally identical processing

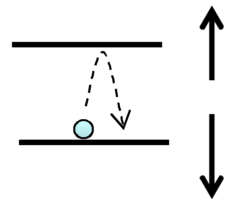

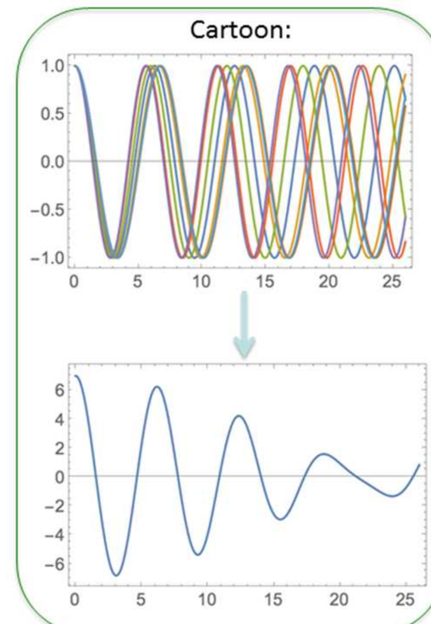

- Coarse metrics of material quality with respect to spin "vacuum" are T2 & T2*
- Roughly, this is a measure of inhomogeneous local B-field from dipoles (T2*) & how rapidly that field is changing (T2)
- This case: ESR: T2 = 0.31 ms, T2* = 10-20 μs

Sandia National Laboratories

Preliminary GST Results

#	Germ
1	Gx
2	Gy
3	Gi
4	Gx · Gy
5	Gx · Gy · Gi
6	Gx · Gi · Gy
7	Gx · Gi · Gi
8	Gy · Gi · Gi
9	Gx · Gx · Gi · Gy
10	Gx · Gy · Gy · Gi
11	Gx · Gx · Gy · Gx · Gy · Gy

Gate	Process Infidelity
Gi	0.026748
Gx	0.047344
Gy	0.055106

- Gate set tomography used to characterize rotations
- General idea:
  - Provide initial state of unknown "quality"
  - Provide measurement of unknown "quality"
  - Apply sequences gates and idles
  - Results characterize gates and SPAM errors

- Maximum length concatenations we used was 8.
- 400 ns pulse times, 1.8 us clock cycle, 100 kHz BW on read-out
- SPAM error of order 6% & Idle error ~3%
- X/Y rotations are of order 4-5% error. Looks like phase error between X and Y
- Order of 1 % uncertainty in infidelity estimates

Blume-Kohout, Nielsen, Gamble

Dimer Observation & Motivation for Single Donor Placement

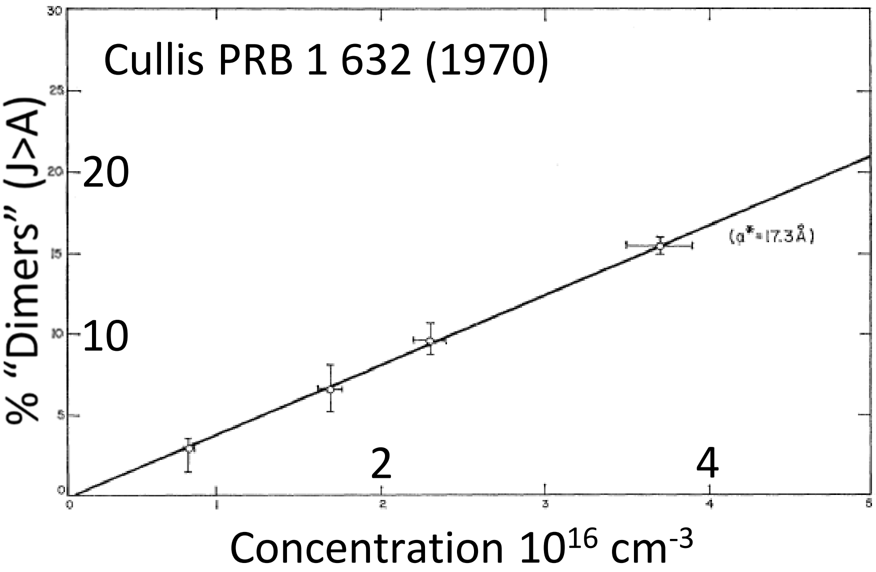

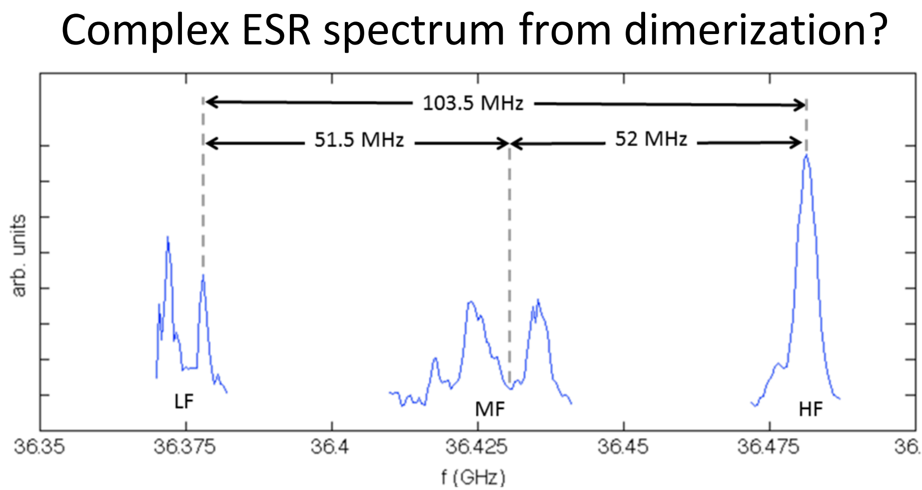

- Often assumed that single donor placement necessary for reasonable two qubit path
- Timed implant combined with tunable D-QD coupling would relax this strict requirement
- Down side of timed implant – the others can still introduce undesired effects
- Precision placement of single donors still the way to go
- Higher yield and performance path (long term view)
  - Place one and know you have one in zone
  - Better QD lateral shift or D vertical gate

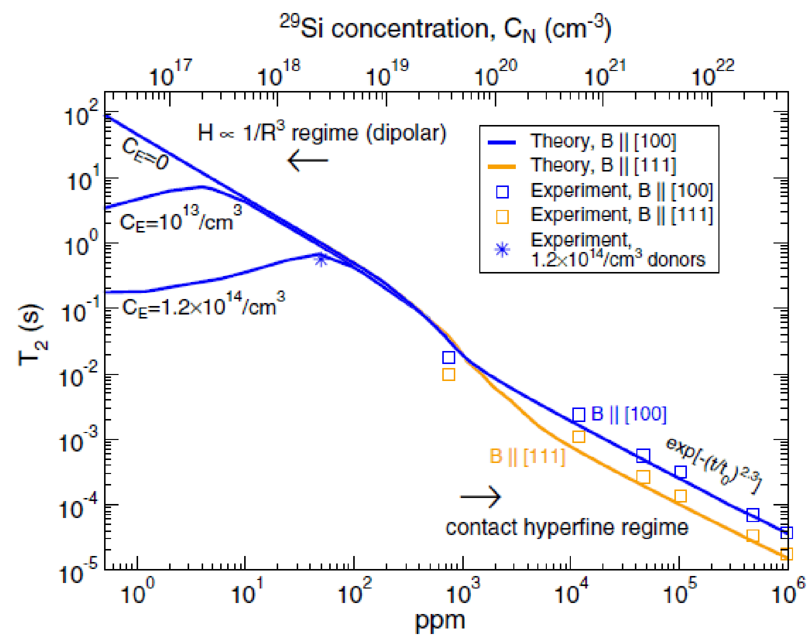

Sandia National Laboratories

Summary of single donor qubit (ESR/NMR)

- 28Si introduced in to local ESR donor qubit fab platform (L. Tracy)
- Line width of ~30 kHz observed two times
- T2 comparable to previous reports
- Cryo-HEMT circuit used to overcome dry fridge noise and produce high SNR read-out
  - > 90% fidelity at 100 kHz bandwidth (high SNR)
  - Video-like stability plots (100 ksamples/sec)
- Looking in to HEMT and HBT circuits (T. England)
  - HBT has higher gain for same current levels & details of cold noise models are also not known
- Gate set tomography used to characterize fidelity (Nielsen, Gamble, Blume-Kohout)
  - 2-3% SPAM error
  - 4-5% X-Y rotation error
  - Analog source is possible cause of error
- P2 dimer is plausible explanation of complex spectrum observed in natural Si device (Luhman)
  - Modeling of this system highlights how the ESR technique leads to identification of a limited range of consistent parameters => metrology technique for clarifying dimer details
- Developing NMR now

Outline

- Motivations
- MOS single donor ESR qubits (natural & ^{28}Si)
- Two qubit nanostructures
  - Latch read-out for S/T qubits
  - Donor hyperfine driven S/T qubit
    - Coherent donor spin coupling to surface QD
  - New poly Si QD-D design
  - Advanced single donor fabrication (STM – single ion implant)

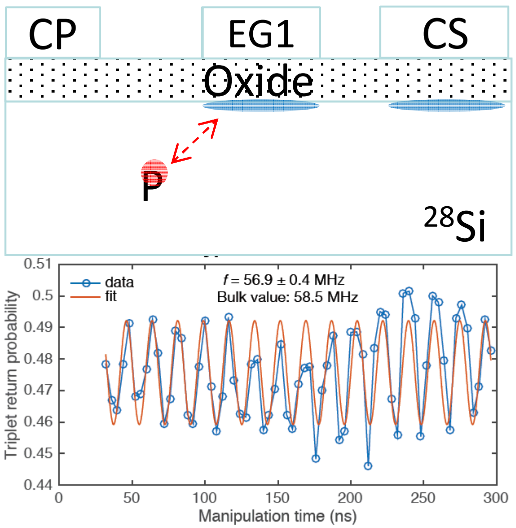

- Summary

Donor-donor coupling concept

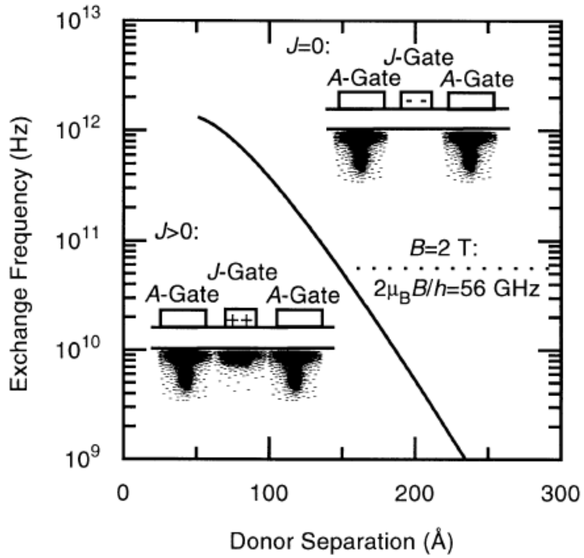

Kane (1998)

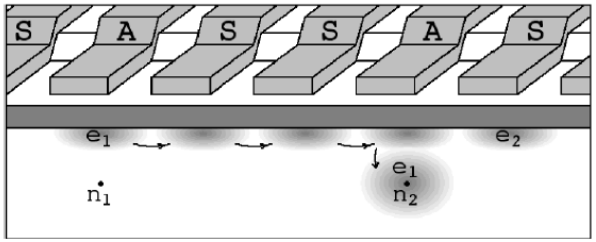

Skinner & Kane (2003)

Also transport: Hollenberg (2007), Morton (2009); Witzel (2015)

- Donors are a great qubit
- Many ideas about coupling donors that use interface
- Very general question that we are presently addressing: can a donor practically be coherently-coupled to something at an interface and can that capability be extended
- SNL: donor coherently coupled to MOS QD recently
- This is a platform to look at these questions

G-factor control

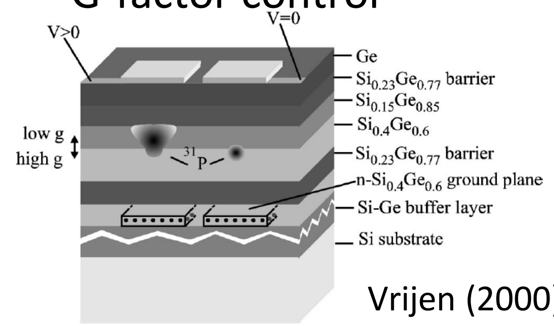

Vrijen (2000)

Approach: couple buried donor to surface QD

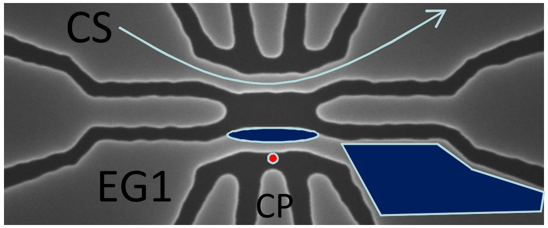

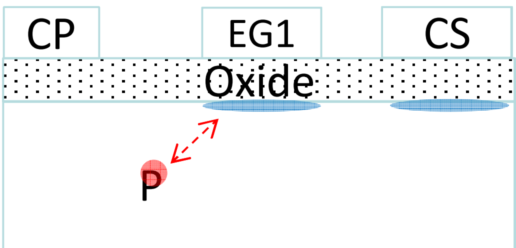

Canonical S/T qubit

$$\hat{H}_{ST} = J(\epsilon)\hat{\sigma}_z + \Delta B_Z(\epsilon)\hat{\sigma}_x$$

Donor-QD S/T qubit → $AI \cdot S$

Qubit Bloch Sphere

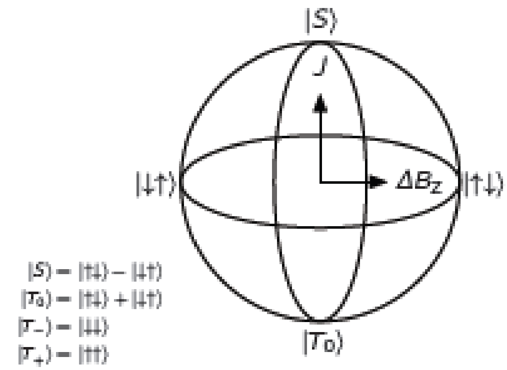

$$\hat{H}_{ST} = J(\epsilon)\hat{\sigma}_z + \Delta B_Z\hat{\sigma}_x$$

- Encode as singlet-triplet qubit
- Rationale for using this choice as test platform:
  - Platform to examine tuning of the charge & dynamics (e.g., tunnel coupling)
  - Produces an appealing two-axis controlled S/T qubit
  - Rotation frequency is chemically distinct
  - Opens up a potential electrical read-out of nuclear spin
  - Directly probes coherence times of surface-bulk-donor coupling

Approach: Couple a N=1 MOS-QD to a Buried Donor

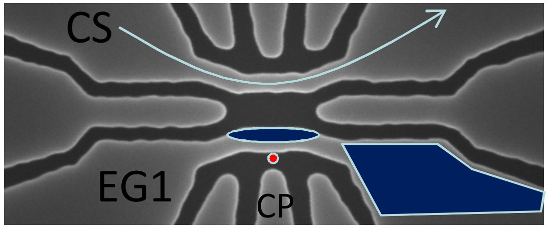

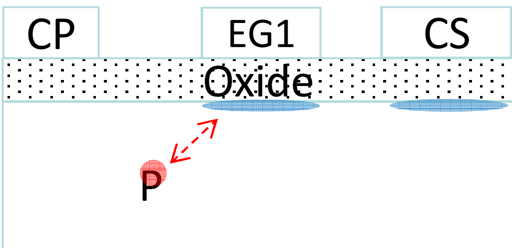

2-spin singlet-triplet qubit

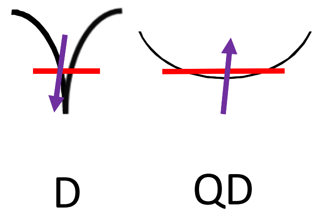

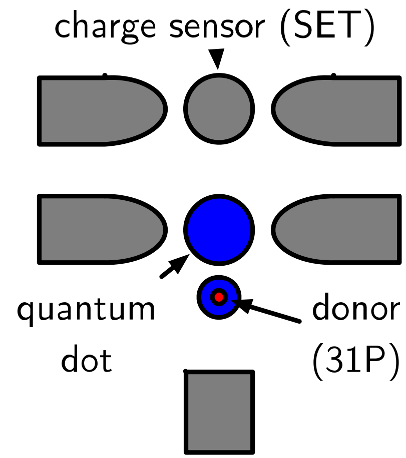

- Extend the single donor qubit lay-out to include a charge sensor
- Charge sensed donor-QD system is now an experimental double quantum dot platform to test the D to surface coupling idea

Approach: Couple a N=1 MOS-QD to a Buried Donor

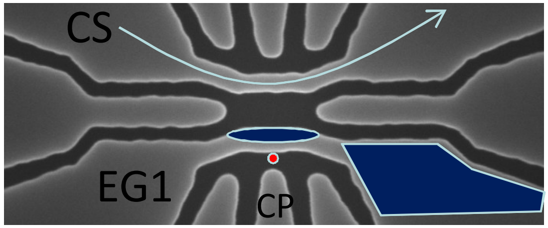

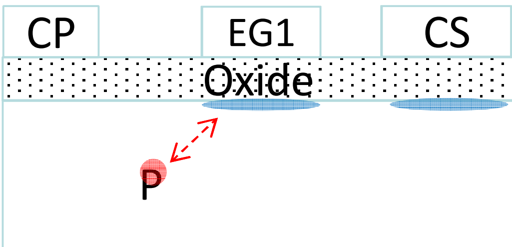

2-spin singlet-triplet qubit

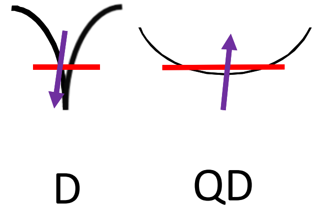

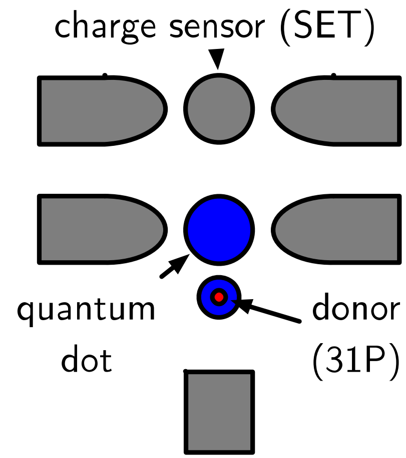

- Extend the single donor qubit lay-out to include a charge sensor
- Charge sensed donor-QD system is now an experimental double quantum dot platform to test the D to surface coupling idea

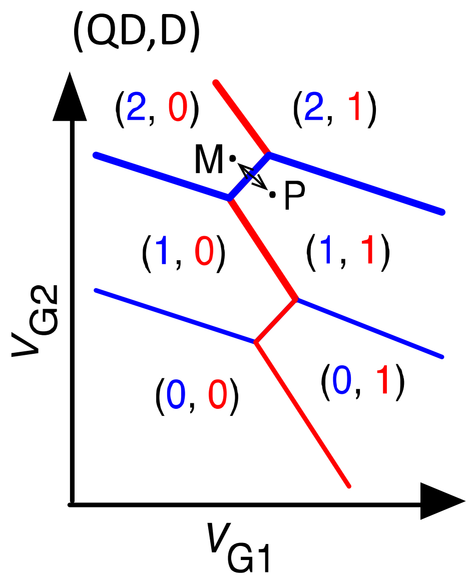

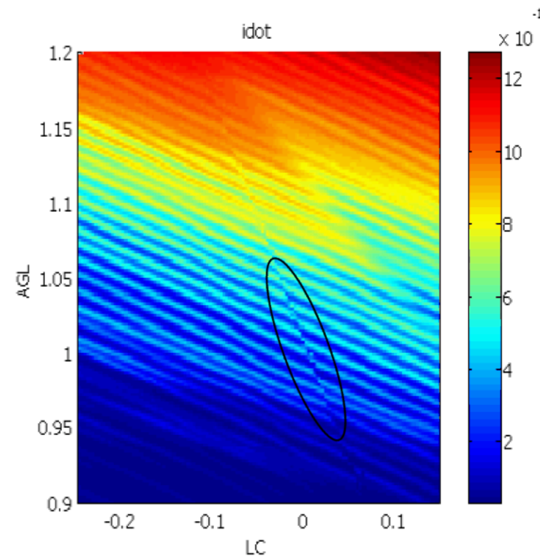

Triangulation of donor position

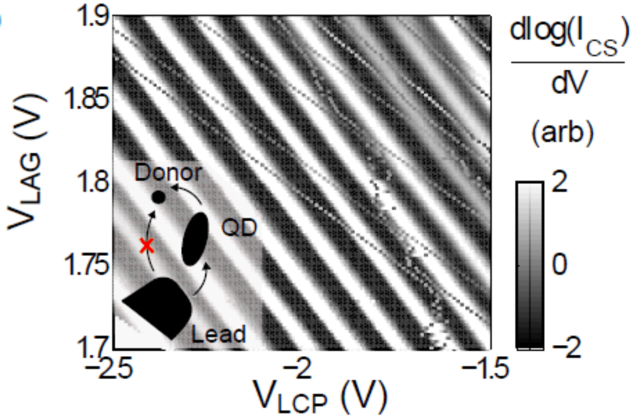

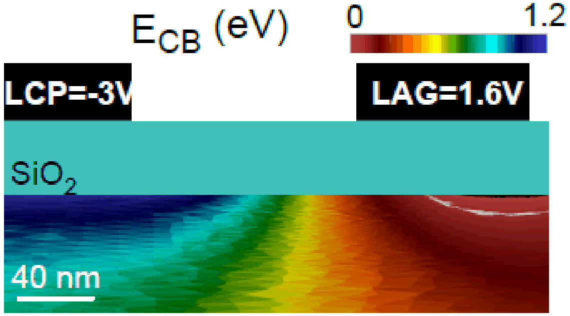

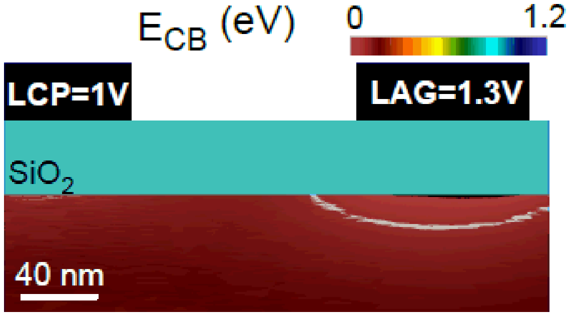

- Modeling of slopes in stability diagrams (against all gates) to help identify position of object
- Capacitances of multi-gate system are sufficient to locate position
- Visible donors are underneath LAG
- Depth/lateral extent of donors:
  - $7 < z < 15$ nm
  - $15 < x,y < 35$ nm
- This observation is also consistent with semi-classical QCAD calculations of 45 meV "ionization contours"

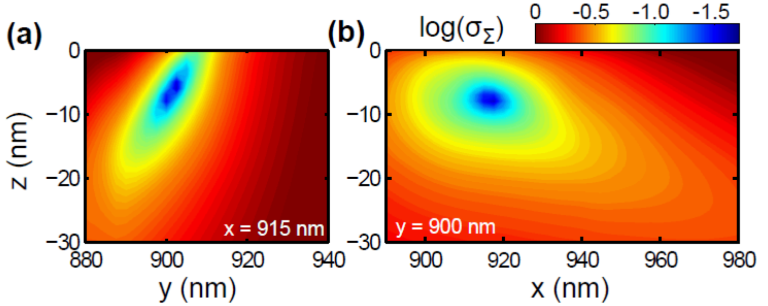

Rudolph et al. (in preparation)

Steps towards coherent control

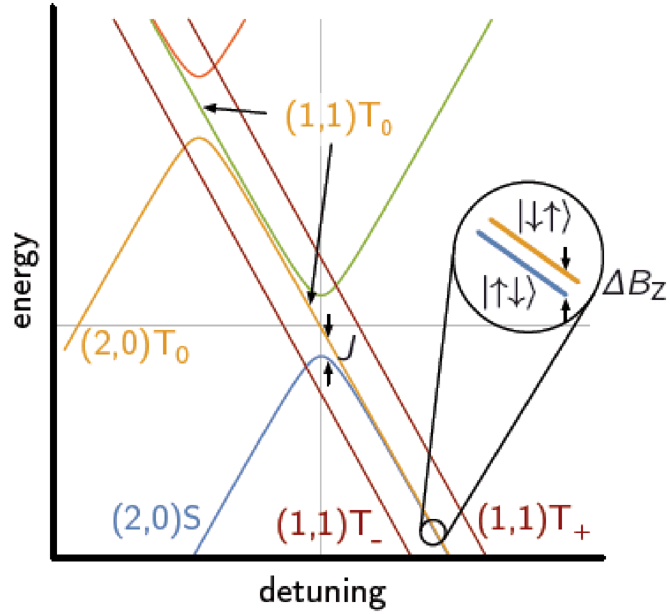

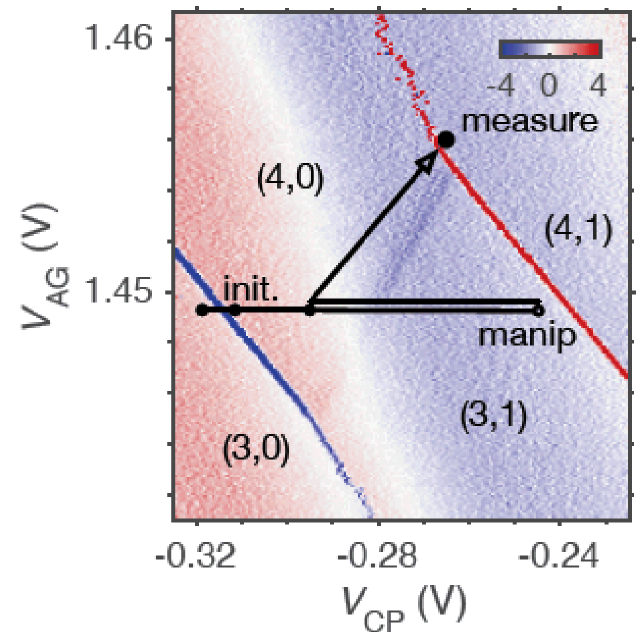

Approach

- Prepare (2,0) singlet
- Pulse into (1,1)
- Ramp rate must be balanced against charge adiabaticity but diabatic relative to J-A anti-crossing
- Shift to higher tunnel coupling through higher N in QD

Poster: Harvey-Collard

Steps towards coherent control

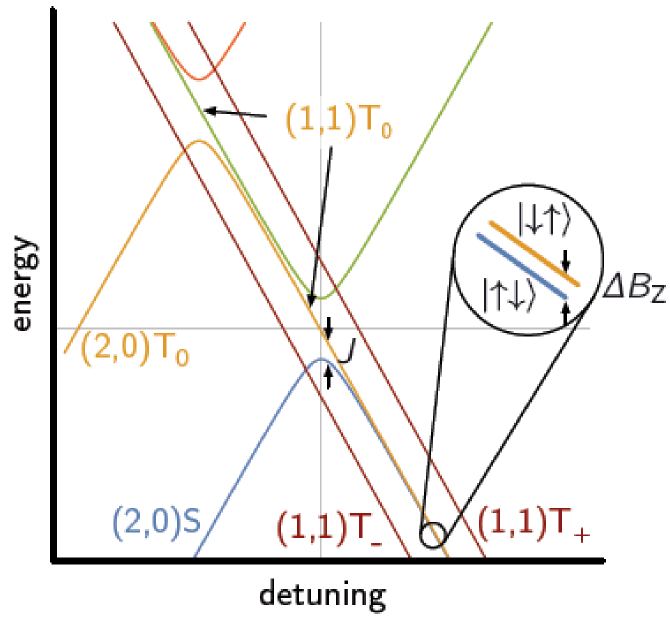

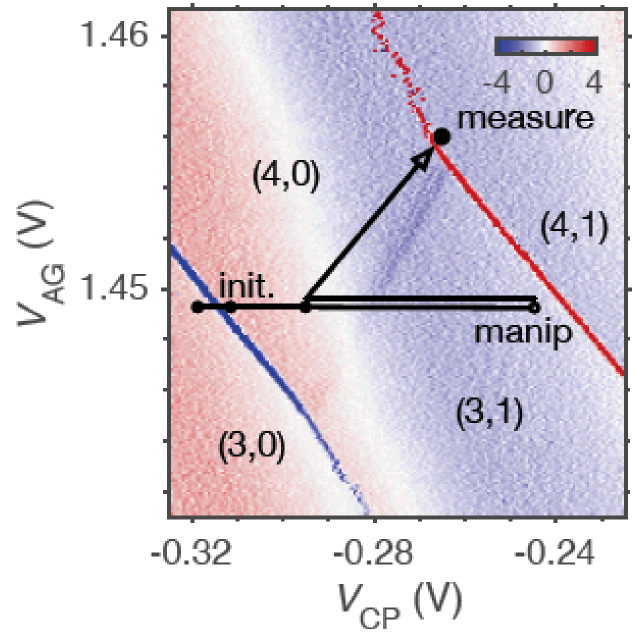

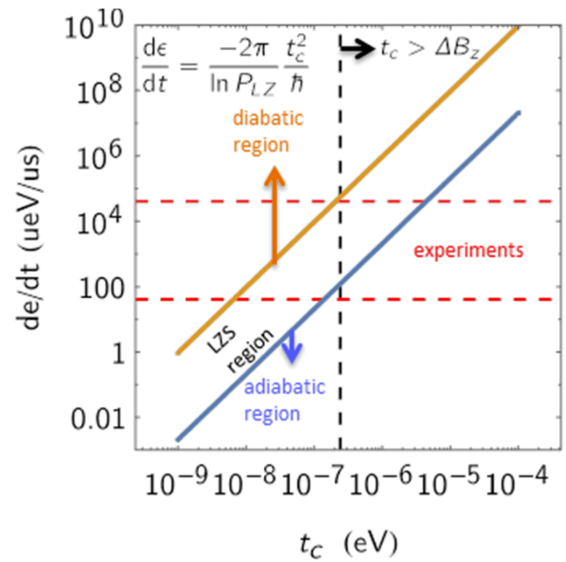

Approach

- Prepare (2,0) singlet
- Pulse into (1,1)
- Ramp rate must be balanced against charge adiabaticity but diabatic relative to the crossing where J < A
- Shift to higher tunnel coupling through higher N in QD

Poster: Harvey-Collard

Pulse sequence & singlet-triplet rotations

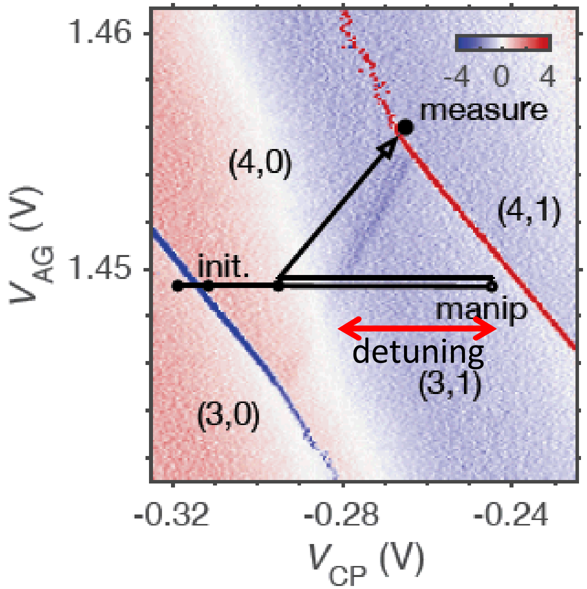

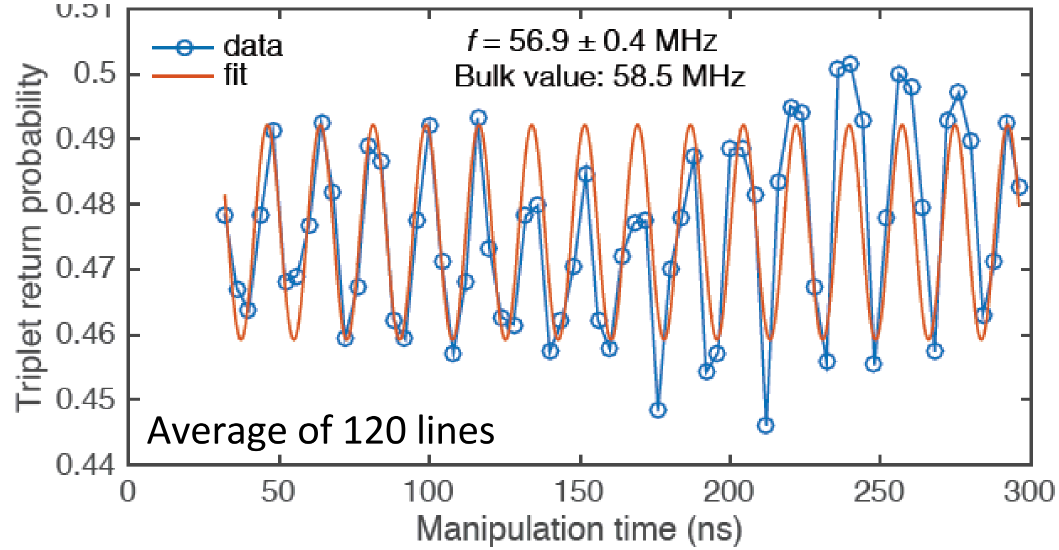

- Coherent oscillations observed for variable time & fixed detuning
  - Note: only the measurement point differs

- Oscillation frequency is close to bulk donor contact hyperfine value of 58.5 MHz
  - Closer to measured single donors in ESR case
- Frequency is detuning dependent – J changes

- T2* order of 1 us from coarse measures at longer times and different detunings

Qubit Bloch Sphere

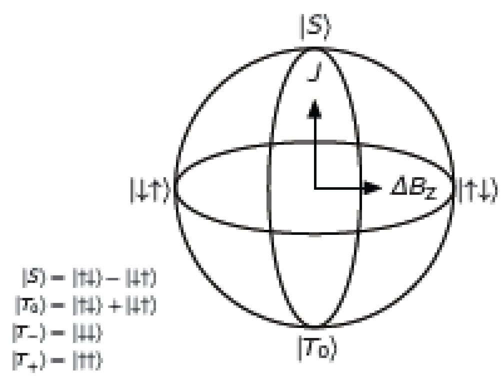

$$\hat{H}_{ST} = J(\epsilon)\hat{\sigma}_z + \Delta B_Z \hat{\sigma}_x$$

Poster: Harvey-Collard

Pulse sequence & singlet-triplet rotations

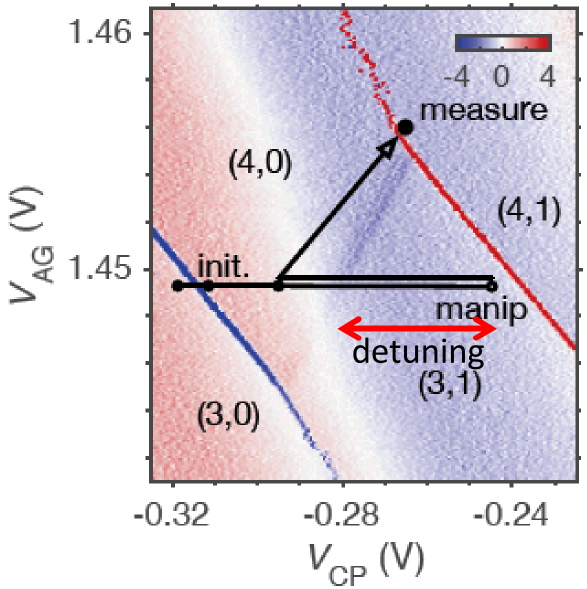

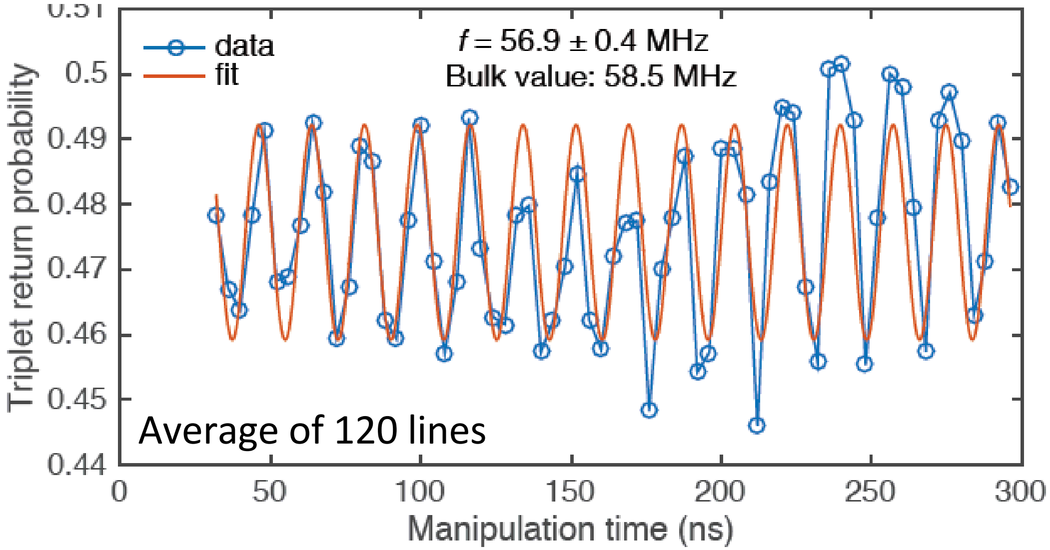

- Coherent oscillations observed for variable time & fixed detuning
  - Note: only the measurement point differs
- Oscillation frequency is close to bulk donor contact hyperfine value of 58.5 MHz
- Frequency is detuning dependent – J changes
- T2* order of 1 μs from coarse measures at longer times and different detunings

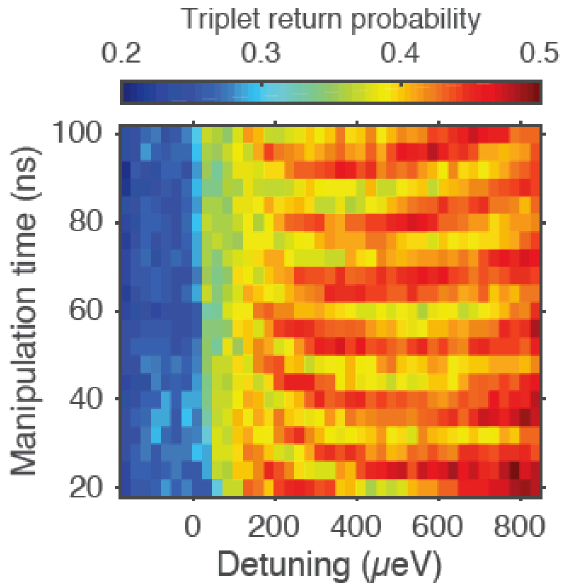

Poster: Harvey-Collard

Comparison to numerical simulation

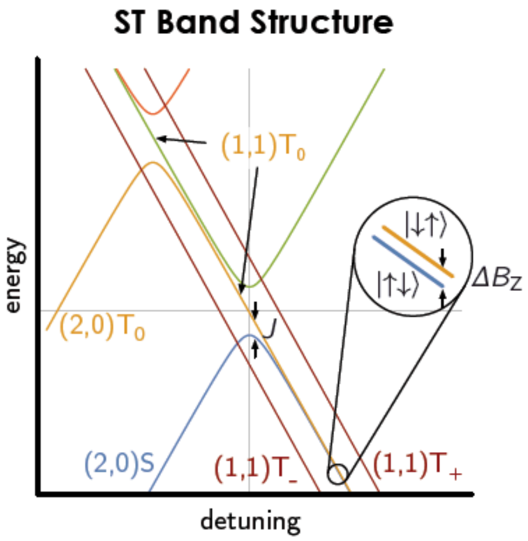

- Phenomenlogical Hamiltonian solved for relevant detuning range
- Dynamics of master equation solved using Lindblad formalism (A assumed, tunnel coupling is fit)
- A number of similar qualitative and quantitative behaviors are exhibited
  - Singlet state is preserved until it is moved to the (1,1) charge state
  - Deeper detuning target reduces J and rotation rate saturates near expected A/2 value
  - Ramp rates affect the rotations including subtle effects of changing integrated time in high J region
  - Reasonable experimental parameters (some directly measured) provide good qualitative agreement
- All consistent with a contact hyperfine driven singlet-triplet qubit
- MAJIQ: MOS, contact-hyperfine (A), exchange (J), single-nuclear-spin-driven (I), qubit

Jacobson

Comparison to numerical simulation

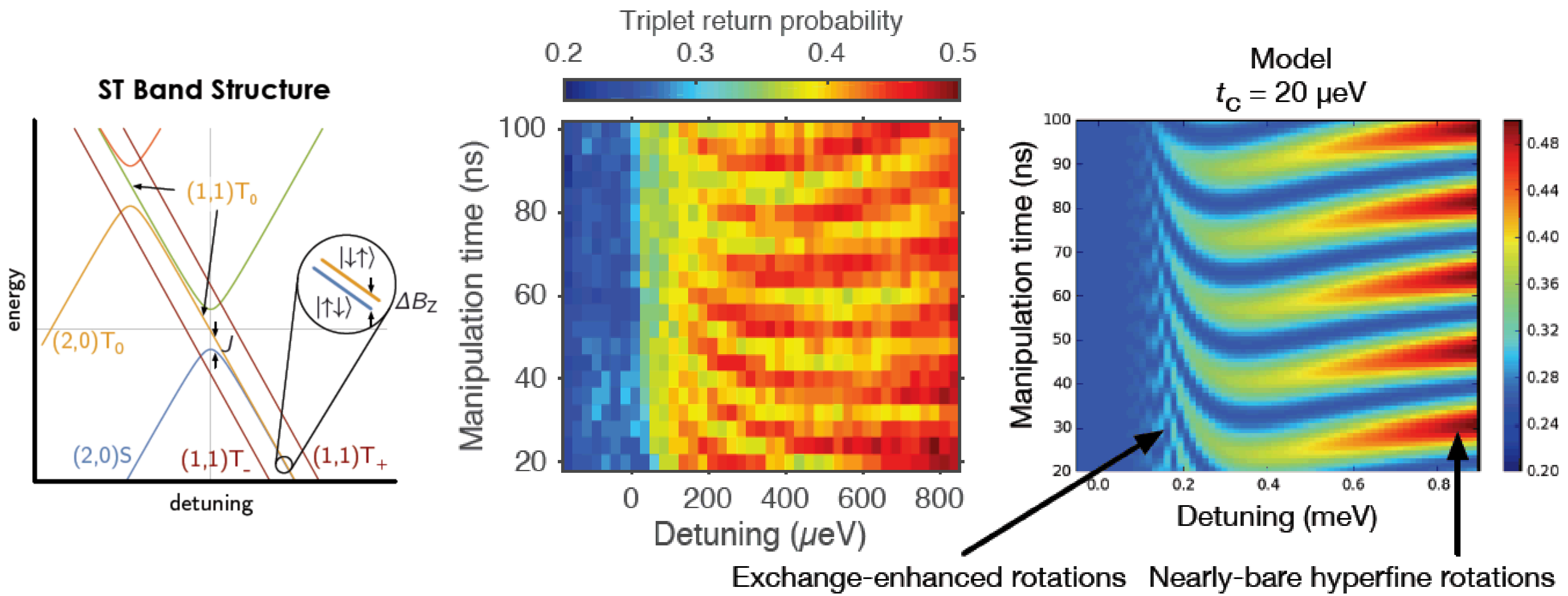

- Phenomenlogical Hamiltonian solved for relevant detuning range
- Dynamics of master equation solved using Lindblad formalism (A assumed, tunnel coupling is fit)
- A number of similar qualitative and quantitative behaviors are exhibited
  - Singlet state is preserved until it is moved to the (1,1) charge state
  - Deeper detuning target reduces J and rotation rate saturates near expected A/2 value
  - Ramp rates affect the rotations including subtle effects of changing integrated time in high J region
  - Reasonable experimental parameters (some directly measured) provide good qualitative agreement
- All consistent with a contact hyperfine driven singlet-triplet qubit
- MAJIQ: MOS, contact-hyperfine (A), exchange (J), single-nuclear-spin-driven (I), qubit

Extended time trace & coarse T2* estimate

- Long time trace. Average of 10 lines.

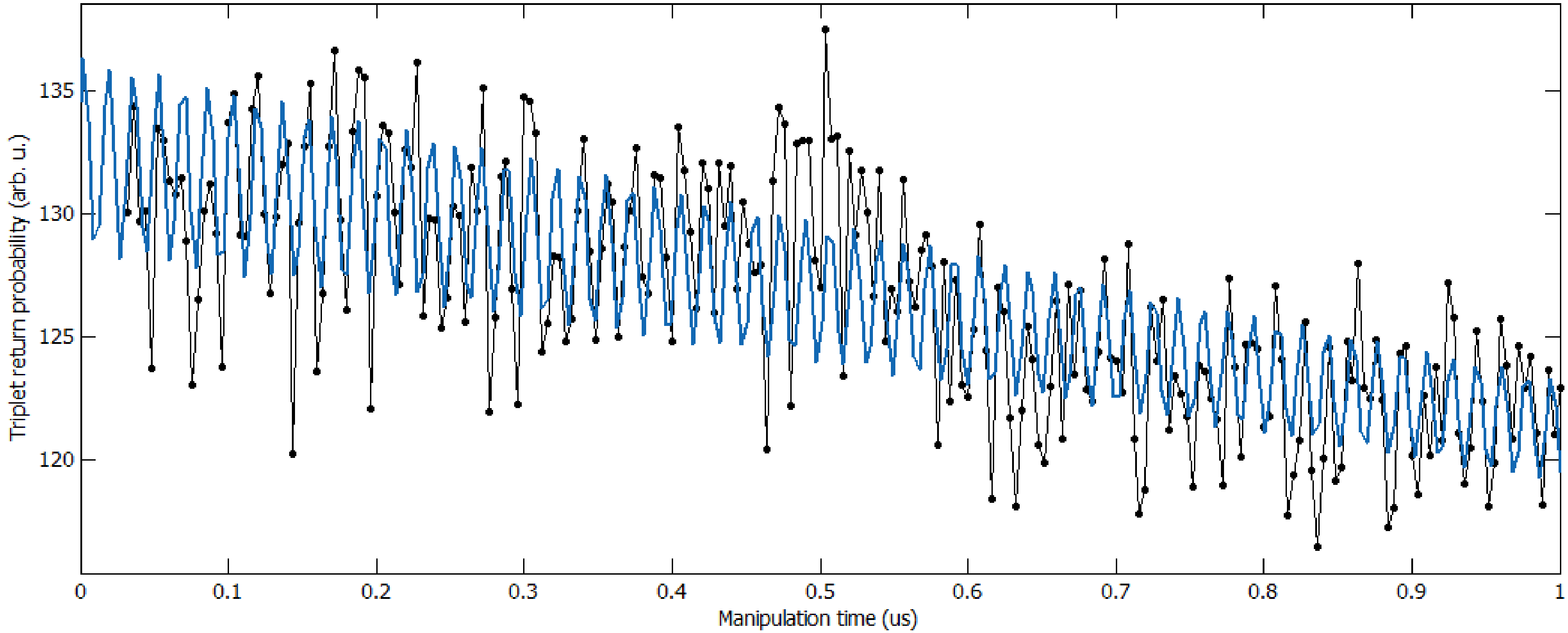

f = 59.5 MHz +- 0.1

T2* = 1.6 +- 0.8 us

Detuning: 897 µeV

Poster: Harvey-Collard

MAJIQ Summary

Short term to do:

- J based rotation
  - "DC" and then look at resonant approaches at ~58 MHz (e.g., similar to Yacoby group)
- Characterize the qubit fidelities and make sure we understand and optimize sources of decoherence
- Slow single shot read-out with latch approach – establish fidelities for that read-out path Explore the T-branch – possibly for nuclear spin read-out
- Different tuning (e.g., different tunnel coupling – different electron number?)

Challenges:

- Tunnel coupling control between D-QD (possible solution in next section)
- Potential bandwidth limits with present version of doped poly (silicide, metal extensions or metal (?))?

Longer term & sci-fi:

- If NMR read-out works – NMR control with "electrical" read-out
- Better design for D-QD (next section)
- Coupling qubits together (more next section)
  - Capacitance, exchange, shuttling(?) …
- Fast single shot read-out (integrate cryo-preamp)
- Higher rotation rate & more nuclear spin flexibility (Sb or Bi)?

Outline

- Motivations
- MOS single donor ESR qubits (natural & ^{28}Si)
- Two qubit nanostructures
  - Latch read-out for S/T qubits
  - Donor hyperfine driven S/T qubit
    - Coherent donor spin coupling to surface QD
  - New poly Si QD & QD-D design
  - Advanced single donor fabrication (STM – single ion implant)
- Summary

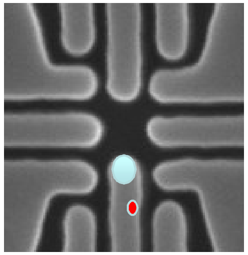

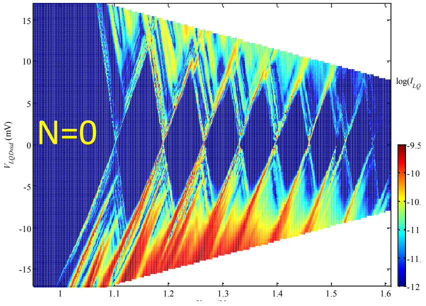

Sandia National Laboratories

The MOS interface

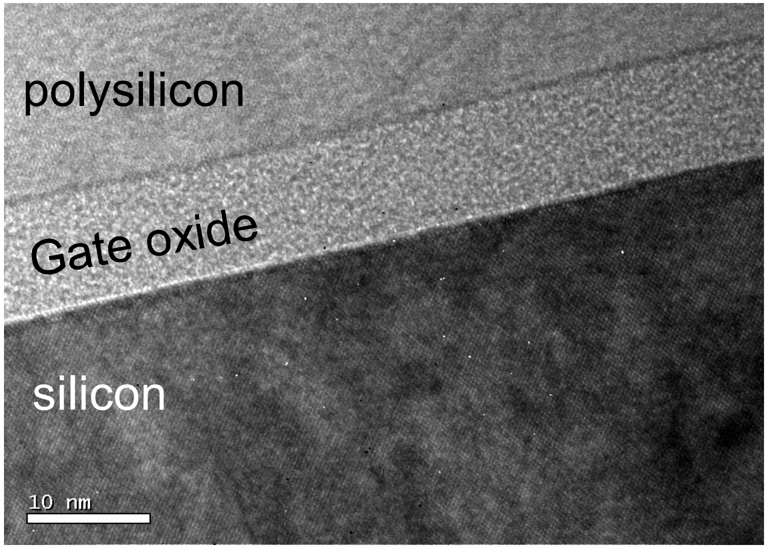

Defects

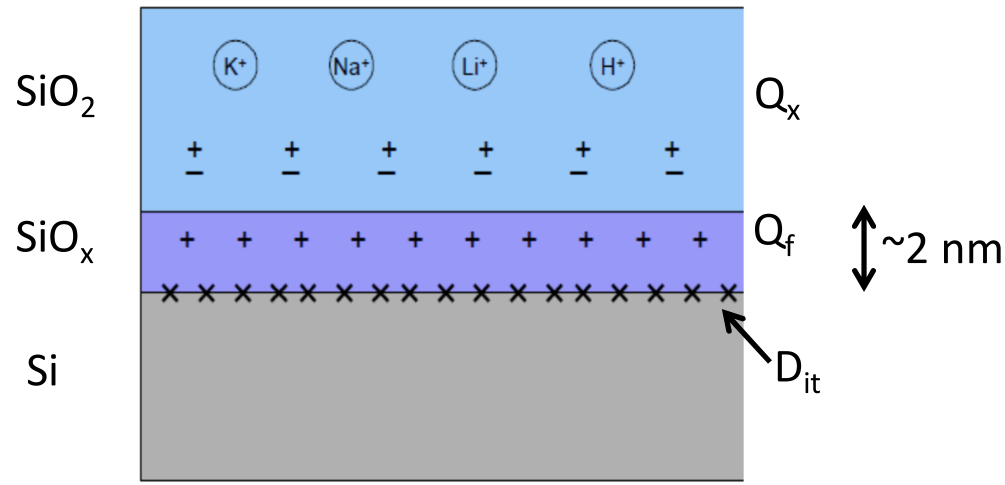

Room temperature picture

- D_{it} Interface traps and border traps within a "tunneling" distance of interface
- Q_f Fixed charge deeper in oxide

Low temperature picture

- Shallow traps are most relevant
- Not much known about interface traps close to band edge
- Fixed charge could be producing a dynamic state at the interface
- Paramaganetic effect on decoherence

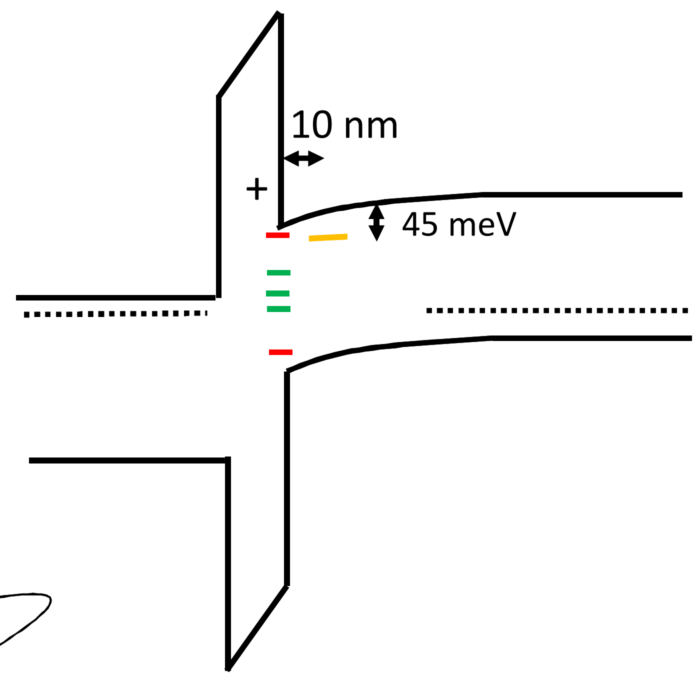

Oxide defect densities

Calculation of unscreened potentials

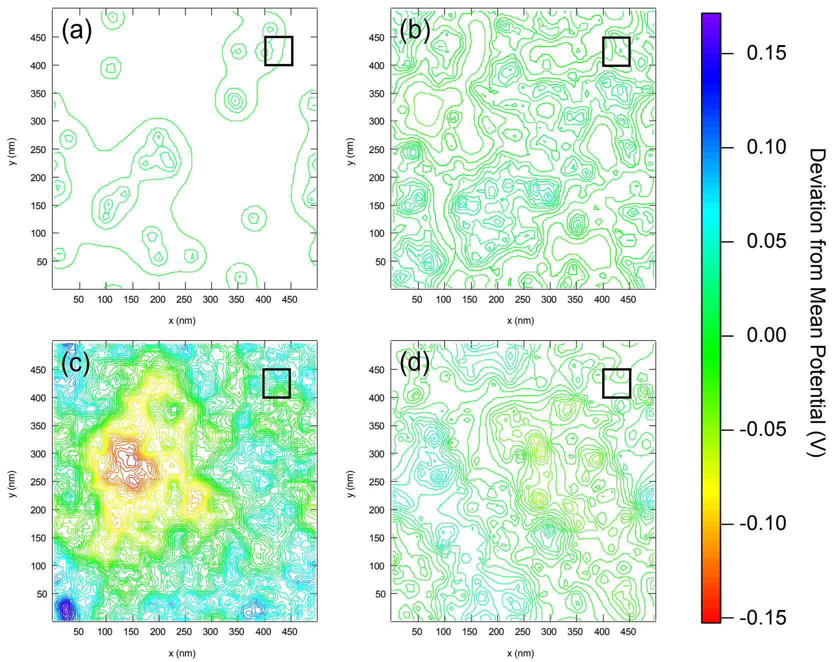

Nordberg et al., PRB 80 115331 (2009)

Electron spin resonance (T ~ 4K)

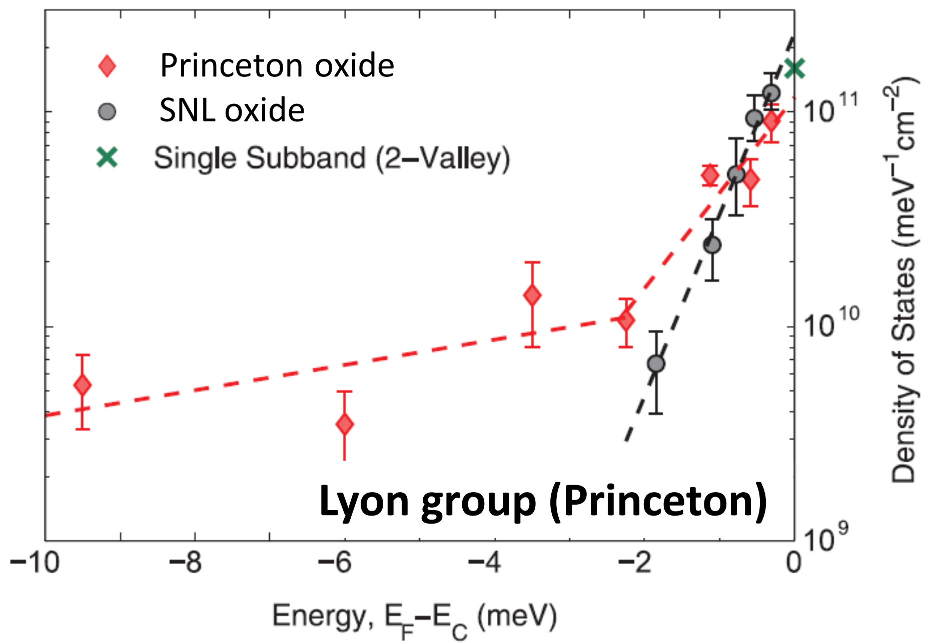

Jock et al., APL 100 023503 (2012)
Rahman et al. PRB 85 125423 (2012) [trap energies]
Pinsook et al., APL (2013) [bandedge DOS]

Calculations would predict substantial "rough" potential
Electrical measurements also suggest a rough potential (e.g., mobility, valley splitting)
Measurements don't always suggest same conclusion – ESR technique vs. peak mobility

New QD design

- Limitations of gated wire design
  - Wire is long (250nm), so transport is difficult through small QD
  - Very asymmetric biasing conditions are necessary for few-electron QD
    - Creates oblong well and preferentially supports a DQD
  - *QD is difficult to physically move*
  - LAG gate has large C to ground, limited BW
  - Extended tunnel barriers susceptible to disorder QD formation

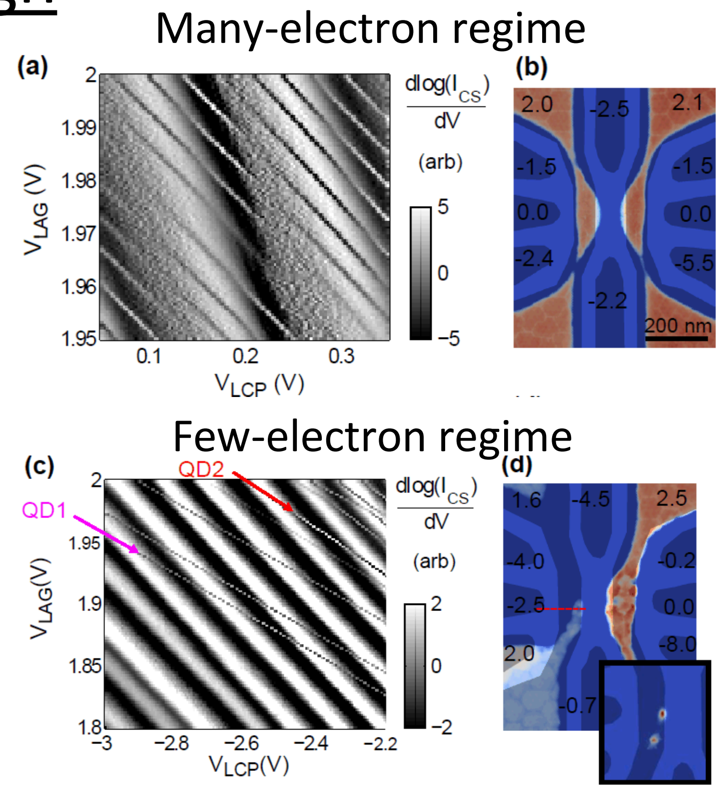

- Community has been moving towards separate reservoir gates
- New design that shrinks dimensions & separates reservoir gates from QD gate
- Separate wire accumulation gates (SWAG)

Gamble, Carroll, Curry, Rudolph

New QD design

- Limitations of gated wire design
  - Wire is long (250nm), so transport is difficult through small QD
  - Very asymmetric biasing conditions are necessary for few-electron QD
    - Creates oblong well and preferentially supports a DQD
  - *QD is difficult to physically move*
  - LAG gate has large C to ground, limited BW

- Community has been moving towards separate reservoir gates
- New design that shrinks dimensions & separates reservoir gates from QD gate
- Separate wire accumulation gates (SWAG)

Many-electron regime

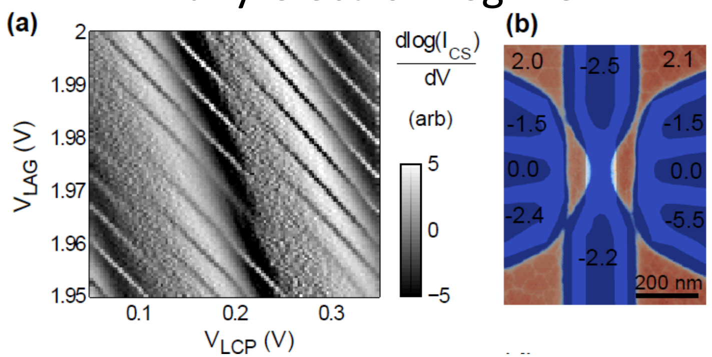

Few-electron regime

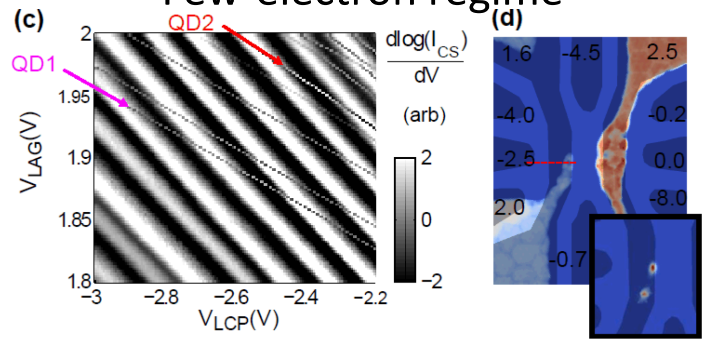

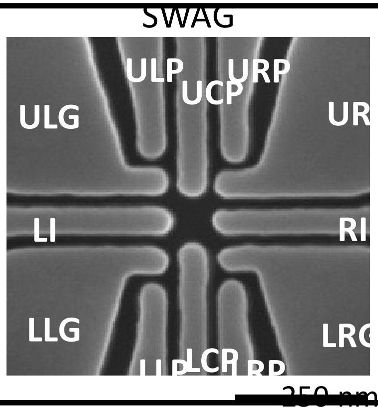

Check for donor transitions

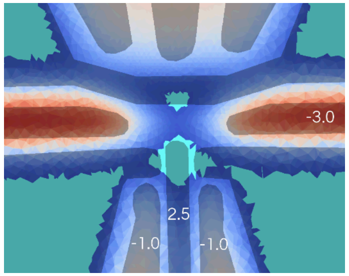

Gamble, Carroll, Curry, Rudolph

Very good and tunable quantum dots in MOS

- Can tune MOS QD to N=1 while keeping both barriers open
- Good charge sense signal from neighboring QD
- Stable or can be tuned to stable regions
- Hypothesis: design is central to controlling the potential at the interface with small enough spatial resolution
- Still a good topic – can we do better?

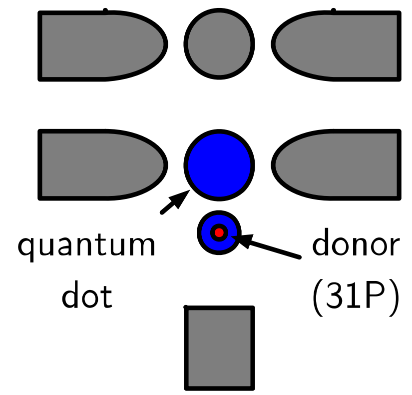

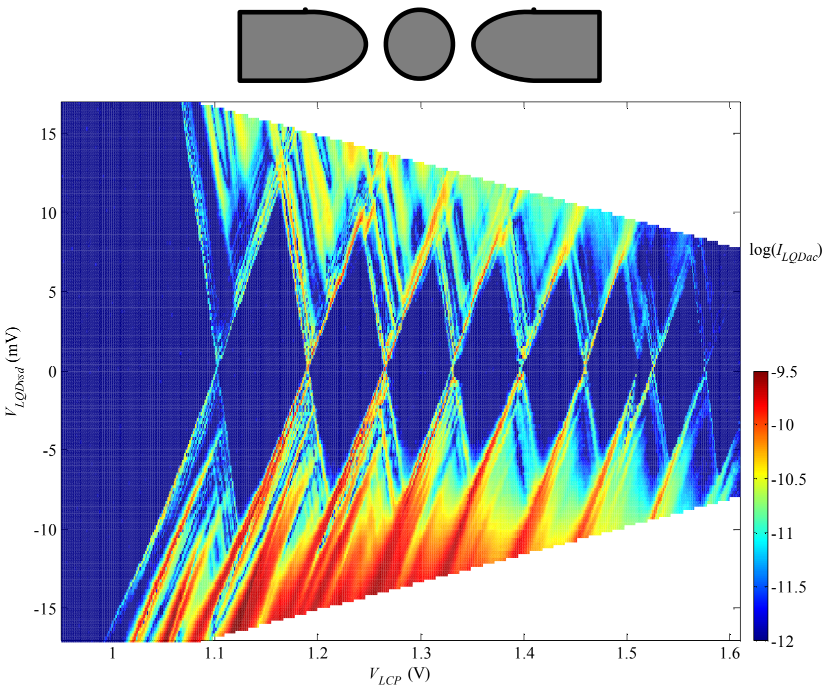

Transport

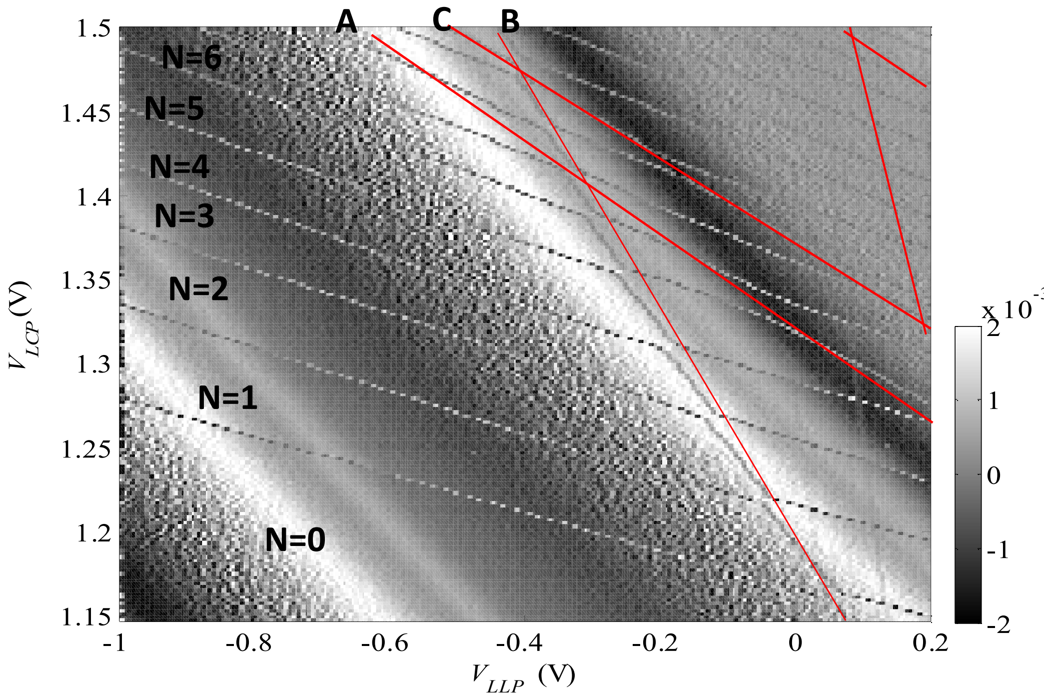

Possible future lay-out for two-qubit coupling

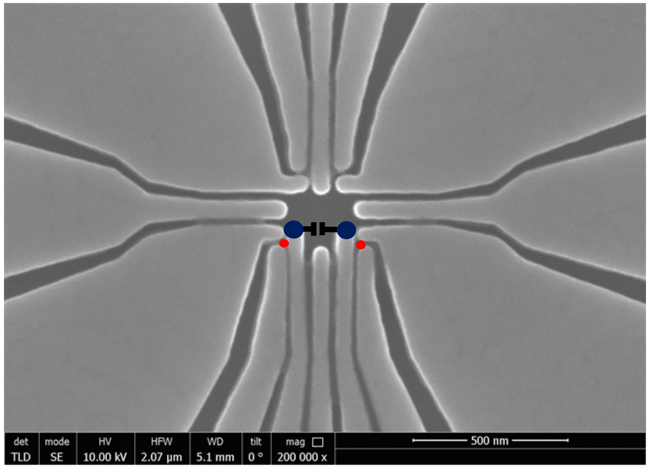

S/T qubit (dB for 2nd-axis)

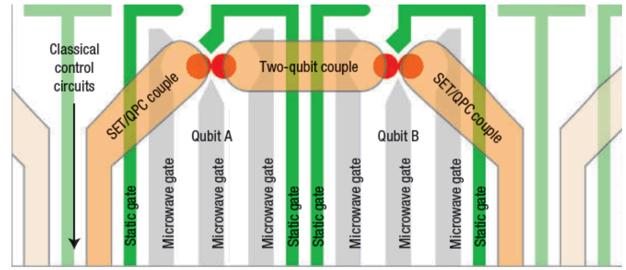

Taylor (2005); Levy (2009); Trifunovic (2013)

Capacitance coupling of MAJIQ-SWAG

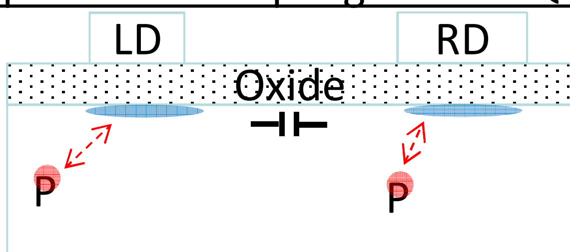

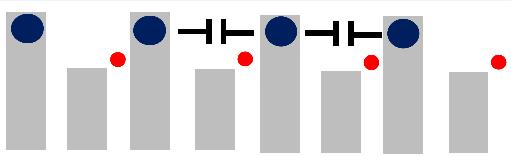

- Capacitance coupling by proximity for two qubit gate
- Approach uses energy selection of one of many donors in an ensemble & poly self-alignment
- Concept might be generalized to more (in a 1D line)

Possible future lay-out for two-qubit coupling

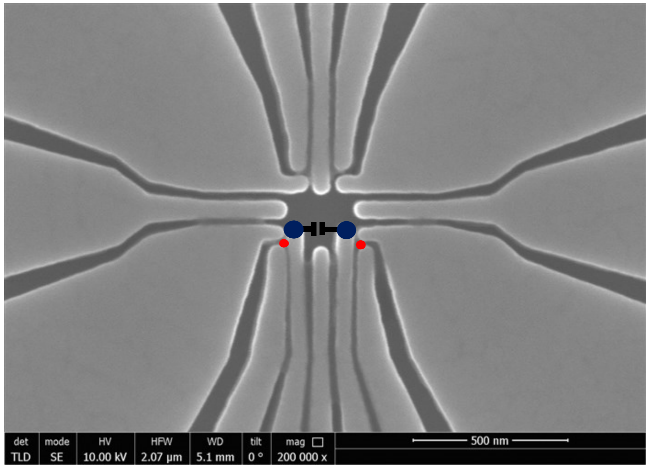

... and other approaches (J or shuttle)

Exchange gate mediated by DQD

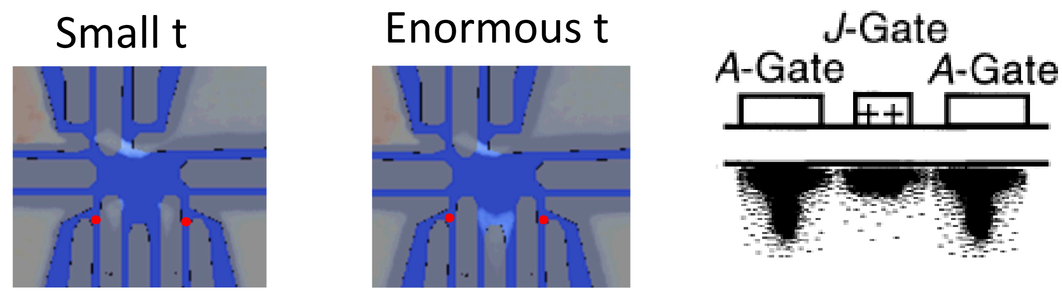

Capacitance coupling of MAJIQ-SWAG

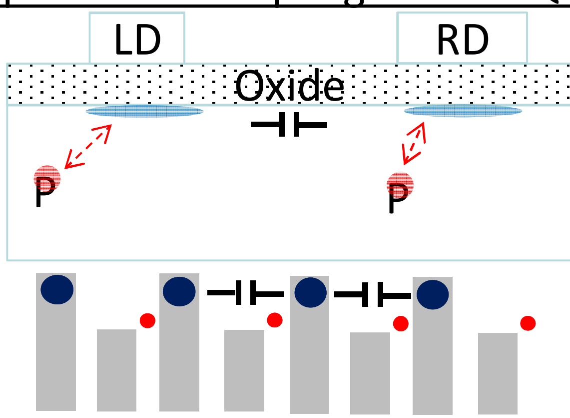

Transport mediated by QDs

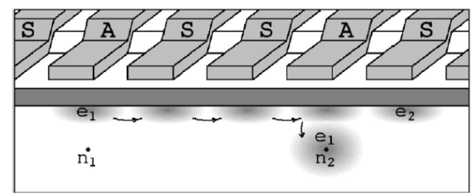

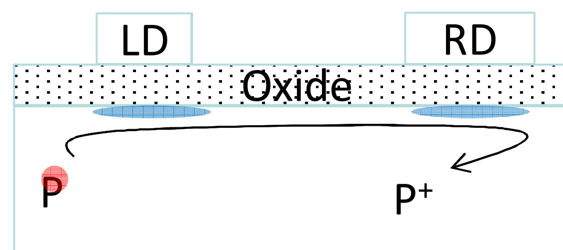

- Capacitance coupling by proximity for two qubit gate
- Approach uses energy selection of one of many donors in an ensemble & poly self-alignment
- Concept might be generalized to more (in a 1D line)

Summary of SWAG & MAJIQ-SWAG

- The gated wire design has important limitations so a new design was developed (separate wire accumulation gate – SWAG)
- Central idea was to move to approach similar to many in the community, separate the reservoir gates. This produces a much more compact device with more tunability down to N=1
- Very good single QD behavior is observed
- Tuning with implanted donors is also observed
  - D-QD transitions can be identified at few electron regime
  - Evidence that tunnel coupling between D and QD can be tuned
  - Implication:
    - Hunt-and-peck for "goldilocks" D-QD tunnel coupling might be relaxed
    - Timed implant D-QD structures might be coupled with reasonable yield
- A double quantum dot (SWAG) has been designed to investigate coupling D-QD qubit structures
  - Two neighboring MAJIQ-SWAG coupled by capacitance proximity (Shulman, Science 2012)
  - Also of interest: exchange or transport (this structure opens up a lot of possibilities to consider/pursue)

Outline

- Motivations
- MOS single donor ESR qubits (natural & ^{28}Si)
- Two qubit nanostructures
  - Latch read-out for S/T qubits
  - Donor hyperfine driven S/T qubit
    - Coherent donor spin coupling to surface QD
  - New poly Si QD-D design
  - Advanced single donor fabrication (STM – single ion implant)
- Summary

Offsets in counted implanted devices (~50% yield)

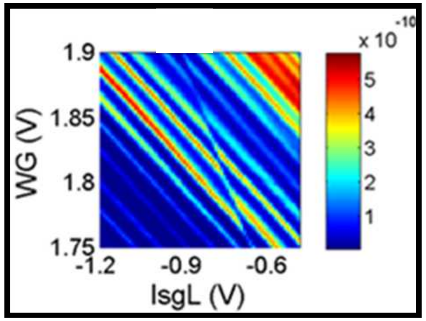

Ultimate lateral and vertical control of donors

1. Start w clean Si(001)

2. Adsorb H resist
Self-limiting 1 monolayer

3. Pattern w STM
Atomic-precision

4. Adsorb PH_3

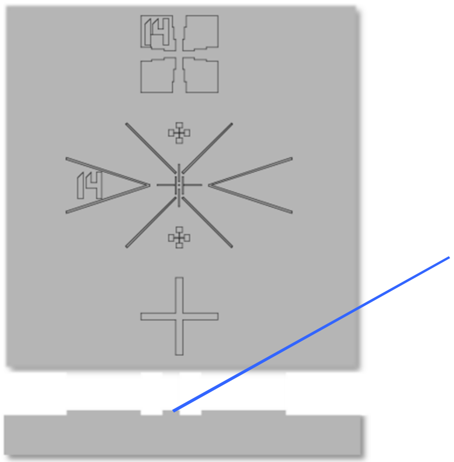

Etched alignment marks

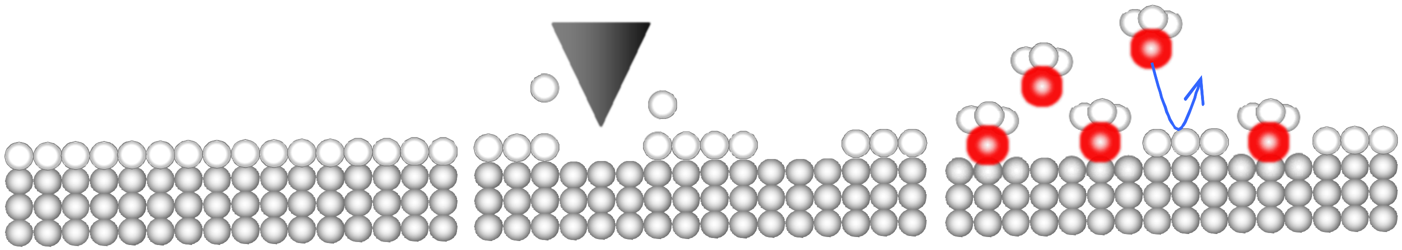

Field emission mode tunnel barrier

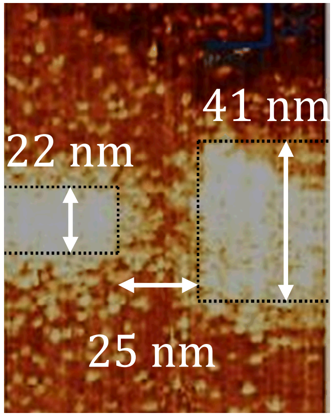

Rudolph [APL 105 163110 (2014)]

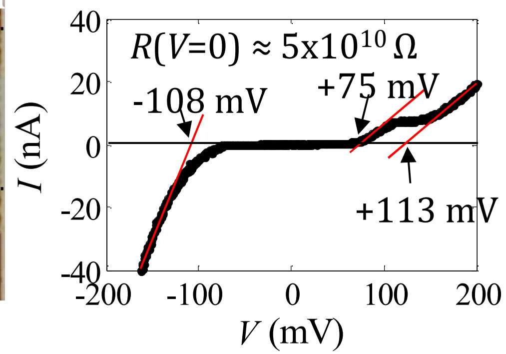

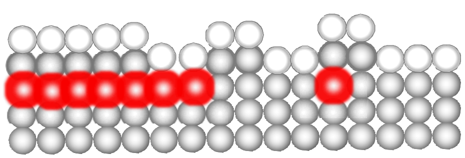

5. Incorporate P
-Anneal→ Si-P swap
-H resist constrains P

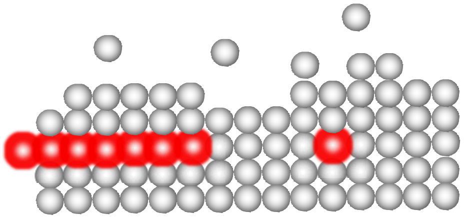

6. Desorb H & bury P in Si

Detector and nanostructure Integration

Single Ion Implant Approach

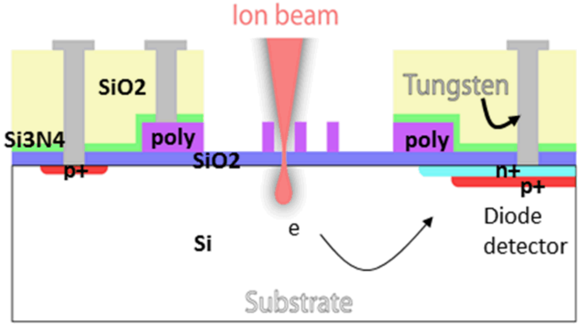

Single Ion Detectors

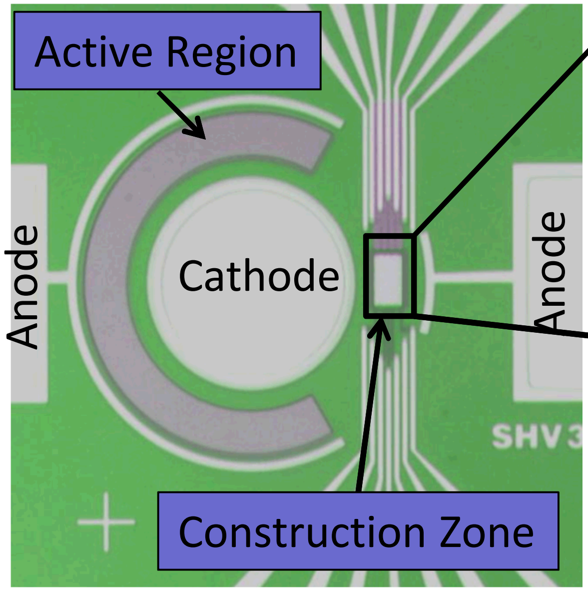

Nanostructures

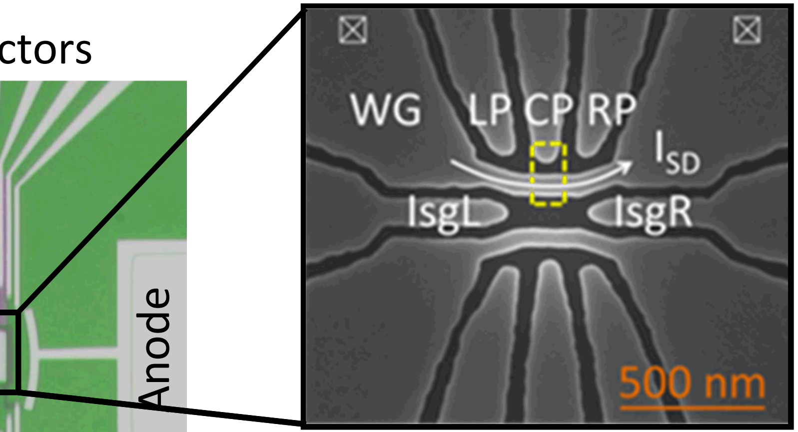

Implant system at Sandia National Labs

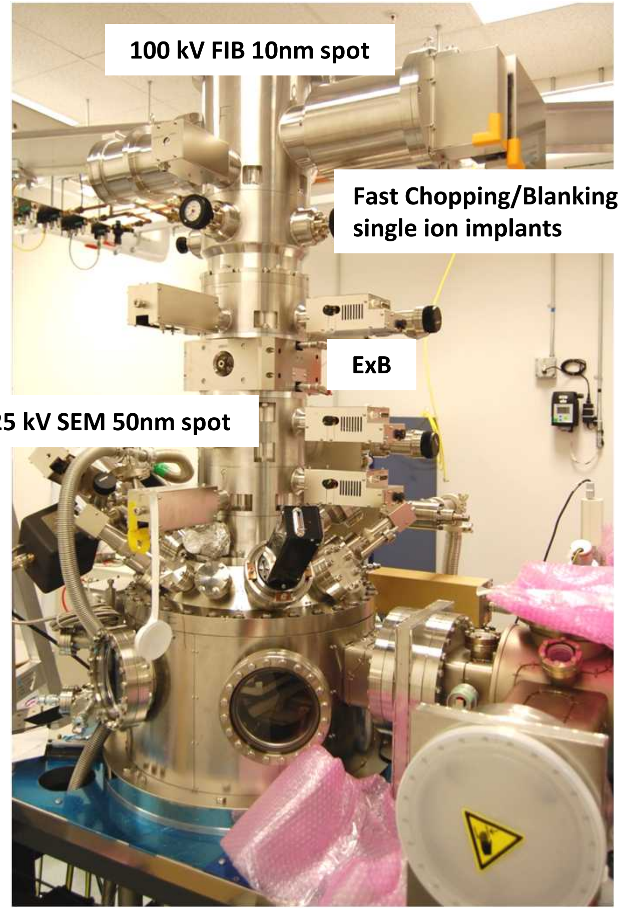

- NanoImplanter (nI)
  - Variable Energy 10-100 kV
  - Liquid Metal Alloy Ion Source (LMAIS)
    - Sb, P, Si, Ga
  - Mass Velocity Filter to pick out ion of interest
  - Fast Blanking and Chopping for single ion implants
  - Demonstrated
    - 10 nm 100 keV Ga^+
    - ~20-30 nm 200 keV Si^{++}

- Beam Spot Size depends on
  - $\Delta E/E$ spread
    - Ion Mass ($\propto m^{1/3}$)
    - Accelerating Voltage ($\propto E^{1/3}$)
  - ***Expect 20-30 nm spot at 30 keV Sb^+***

Detector and nanostructure Integration

Single Ion Implant Approach

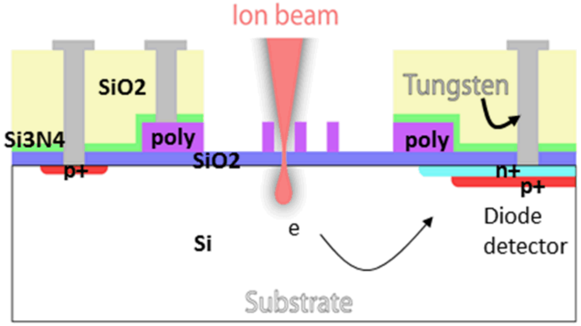

1 ion @ 120 keV Sb / pulse

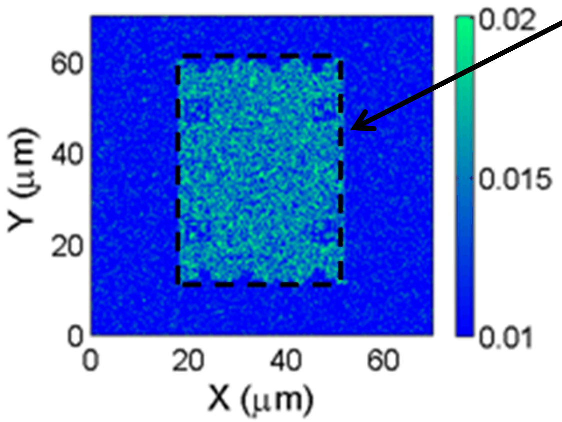

Single Ion Detectors

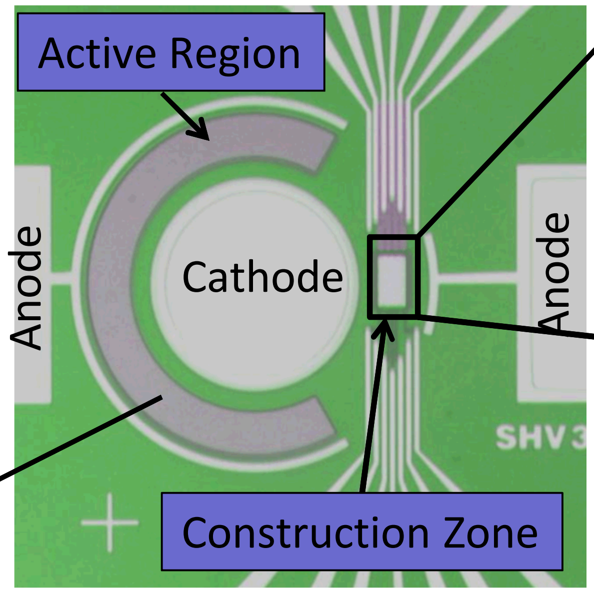

Nanostructures

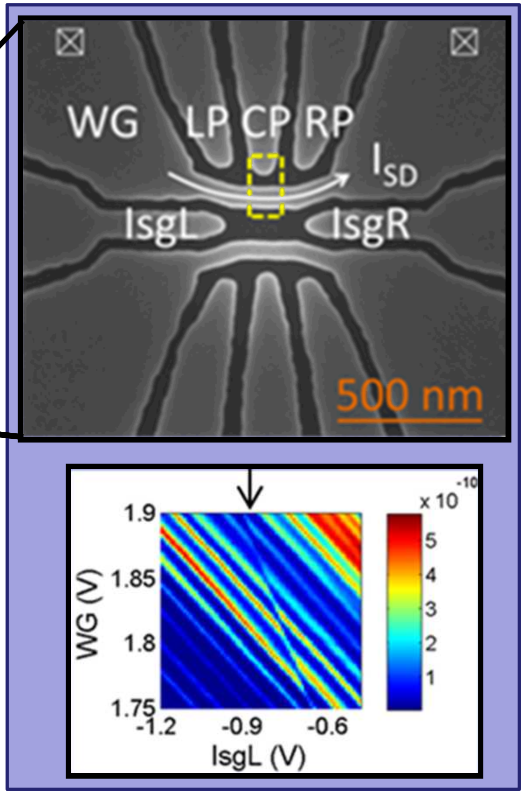

Meenakshi Singh

Successful Integration

❖ Phosphorous Donor Implants

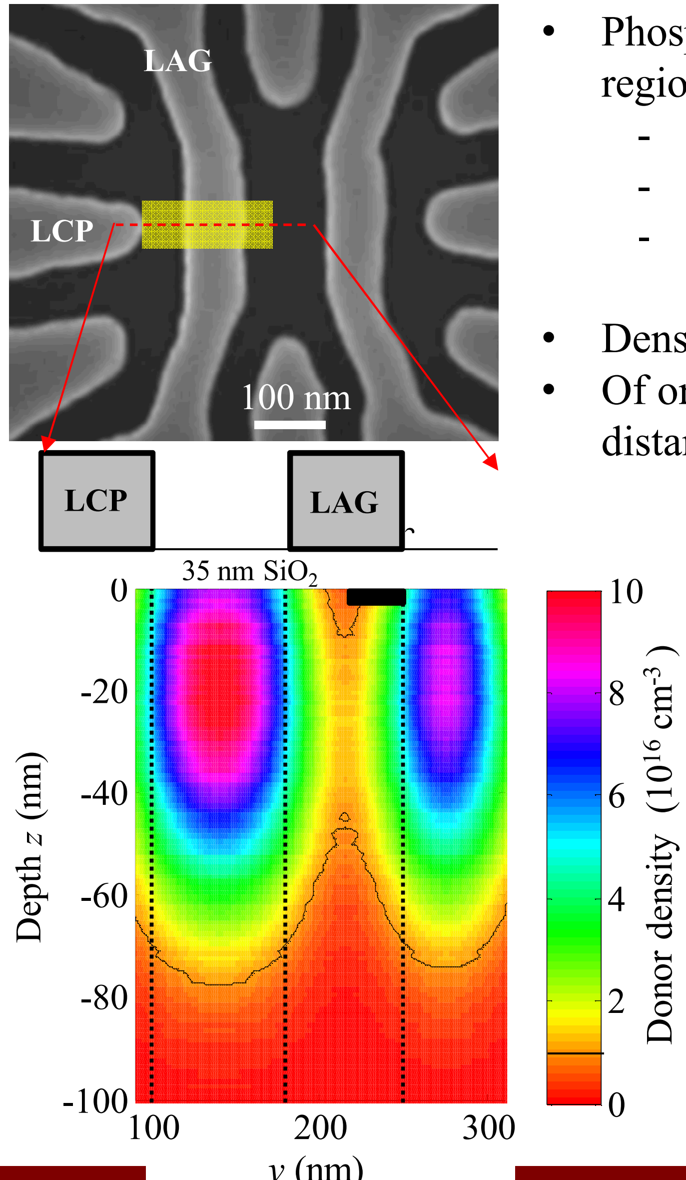

- Phosphorous implanted into yellow region
  - Self-aligned to the poly-Si gates
  - 45 keV
  - 8×10^{11} cm^{-2} fluence (~80 donors)
- Density > 1×10^{16} cm^{-3} under top gate
- Of order 10 donors within the ionization distance from the QD

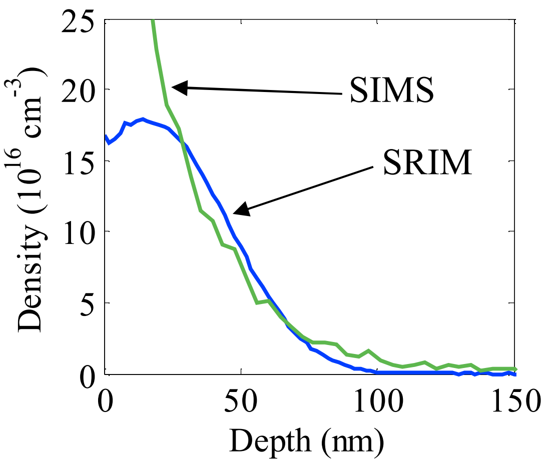

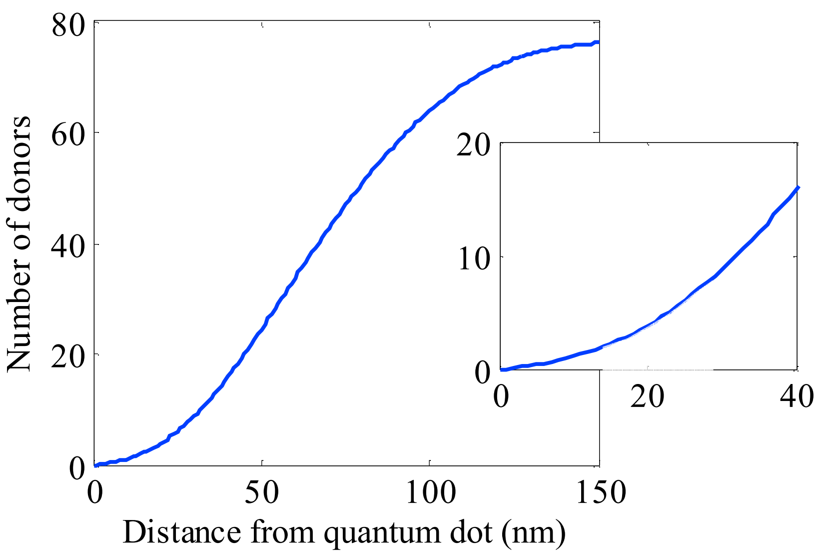

Integration approach: use 35 nm SETs w/ thinned oxide

Last year: 7 nm gate oxide gated wires were not detecting donors
Modeling: 7 nm => donor ionization before good QD formation
New Approach: 35 nm oxide SETs w/ detectors

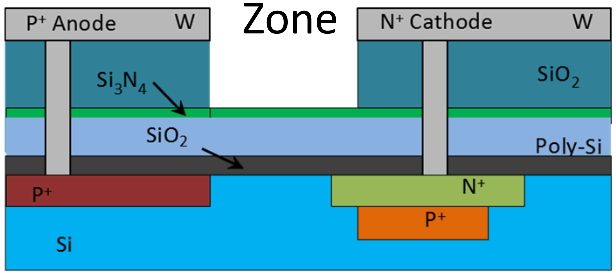

Thin the gate oxide over the donor implant sites to reduce straggle

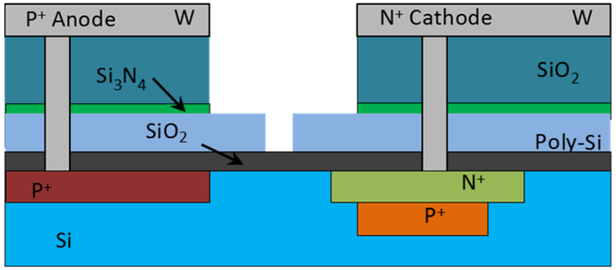

Implantation distributions

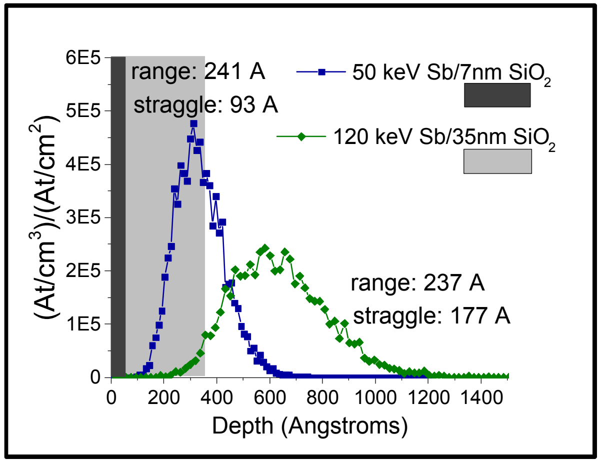

Demonstrated single ion detection in both 35 nm and 35 → 7 nm detectors
Detector improvements this year => 20 keV Sb single ion / pulse detection (SNR=2.5)

Singh & Pacheco
Sandia National Laboratories

Integration approach: use 35 nm SETs w/ thinned oxide

Last year: 7 nm gate oxide gated wires were not detecting donors
Modeling: 7 nm => donor ionization before good QD formation
New Approach: 35 nm oxide SETs w/ detectors

Next: devices & 7 nm thin

Construction Zone

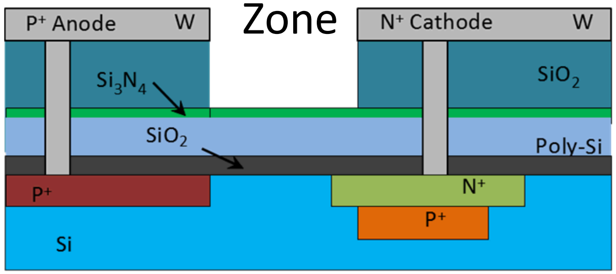

Thin the gate oxide over the donor implant sites to reduce straggle

35 nm

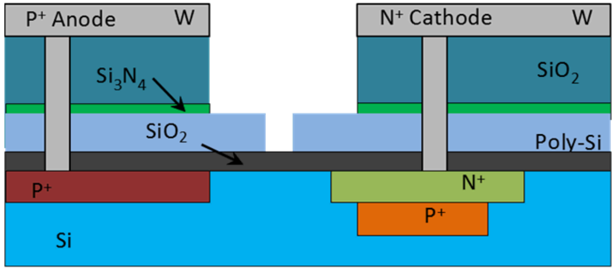

Implantation distributions

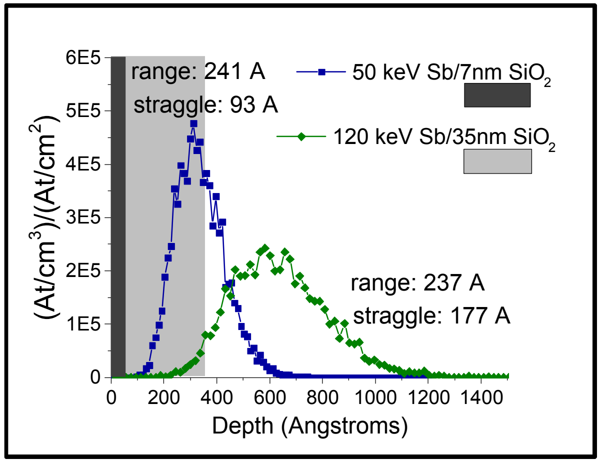

35 → 7 nm

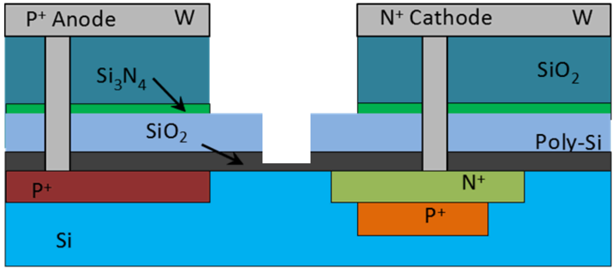

SiO_2 thinned from 35 → 7 nm:

→ Reduce straggle

Demonstrated single ion detection in both 35 nm and 35 → 7 nm detectors
Detector improvements this year => 20 keV Sb single ion / pulse detection (SNR=2.5)

QIST team & external connections

- QIST contributors at SNL
  - **QD & Timed Implant Qubit Fab:** J. Dominguez, R. Manginell, T. Pluym, B. Silva, J. Wendt, S. Wolfley
  - **Qubit control & measurement:** S. Carr, M. Curry, T. England, A. Grine, K. Fortier, R. Lewis, M. Lilly, T.-M. Lu, D. Luhman, J. Rivera, M. Rudolph, P. Sharma, A. Shirkhorshidian, M. Singh, L. Tracy, M. Wanke
  - **Advanced fabrication (two qubit):** E. Bielejec, E. Bussmann, E. Garratt, J. Koepke, A. MacDonald, E. Langlois, M. Marshal, B. McWatters, S. Miller, S. Misra, D. Perry, S. Samora, D. Scrymgeour, R. Simonson, G. Subramanian, D. Ward, E. Yitamben
  - **Device modeling:** J. Gamble, S. Gao, M. Grace, T. Jacobson, R. Muller, E. Nielsen, I. Montano, W. Witzel, K. Young
- Joint research efforts with external community:
  - Australian Centre for Quantum Computing and Communication Technology (D. Jamieson, A. Dzurak, A. Morello, M. Simmons, L. Hollenberg)
  - Princeton University (S. Lyon, J. Petta)
  - NIST (N. Zimmerman, M. Stewart)
  - U. Maryland (S. Das Sarma)
  - National Research Council (A. Sachrajda)
  - U. Sherbrooke (M. Pioro-Ladriere, C. Bureau-Oxton, P. Harvey-Collard)
  - Purdue University (G. Klimeck & R. Rahman)
  - U. New Mexico (I. Deutsch, P. Zarkesh-Ha)
  - U. Wisconsin (M. Eriksson, S. Coppersmith, D. Savage)
  - University College London (J. Morton)
  - Zyvex (J. Randall)
  - Chee Wee (U. Taiwan)
  - McGill (W. Coish, D’Anjou)

Summary

Single spin donor ESR in 28Si

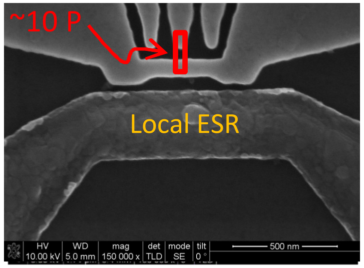

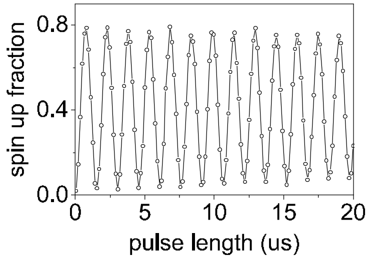

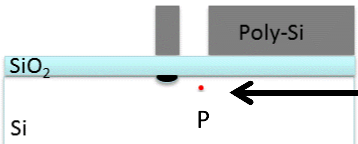

Donor qubit

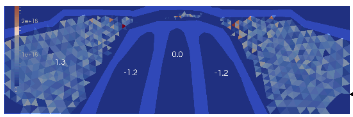

Si QD simulation

MOS S/T qubit driven by single donor

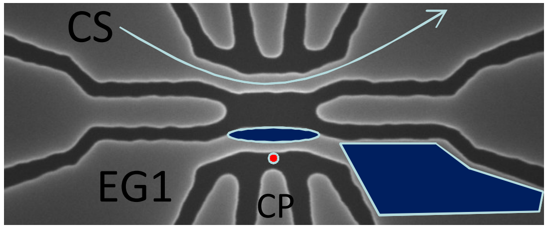

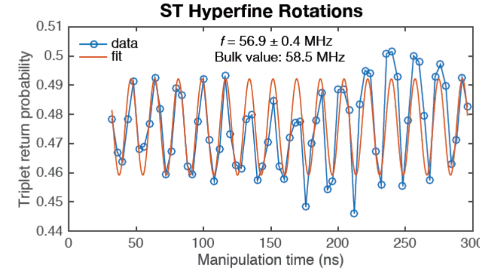

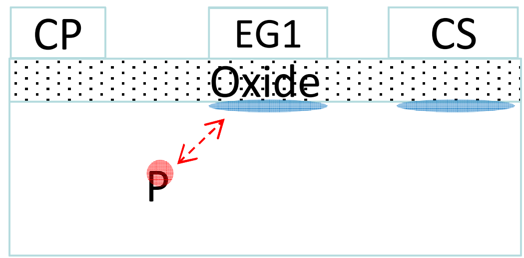

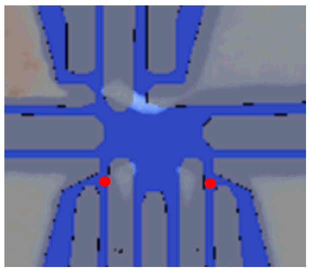

MOS interface

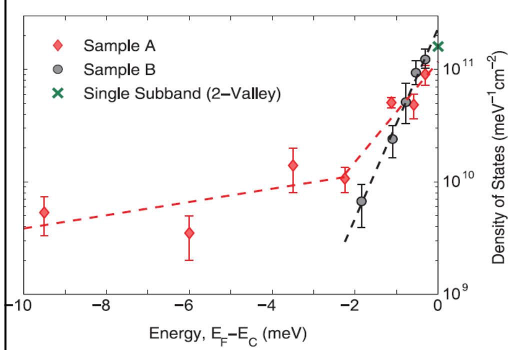

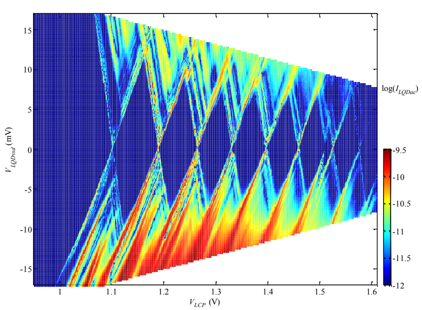

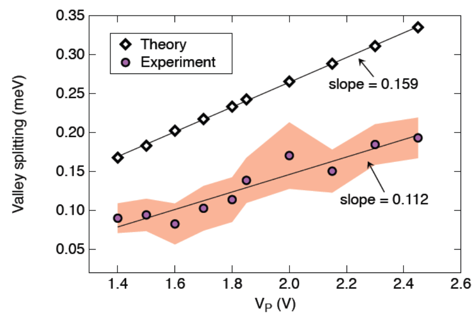

Donor location (SCM)

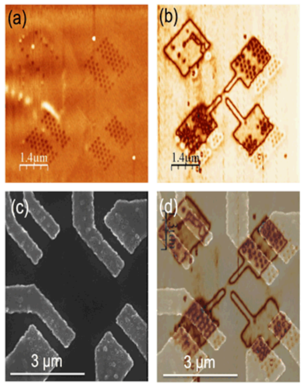

Valley splitting in MOS QD

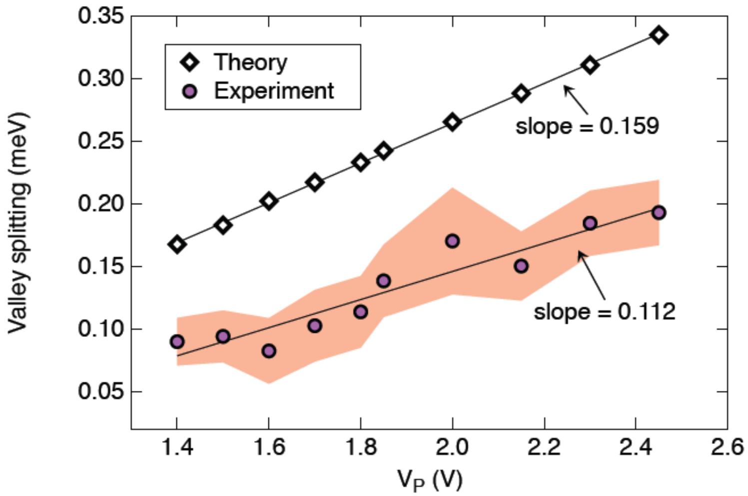

Vertical field

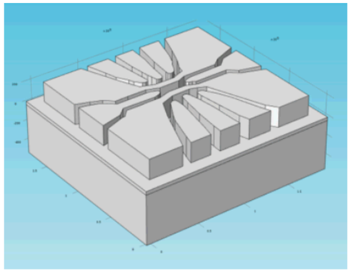

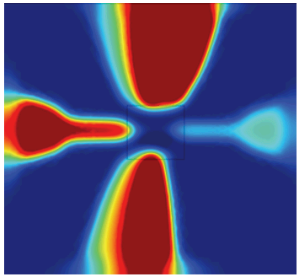

Full 3D calculations to extract vertical field and predicted valley splitting

- The valley splitting is measured using pulsed spectroscopy
  - Measured in multiple MOS QDs with comparable results
- Valley splitting was measured over large range of voltages (i.e., -8 < CP <0)
- Barrier tuned at each location to enable pulsed spectroscopy
- Evs theoretically predicted to go to zero at zero vertical field
- Disagreement between ideal interface model & experiment is being investigated (e.g., disorder, accuracy of threshold, …)

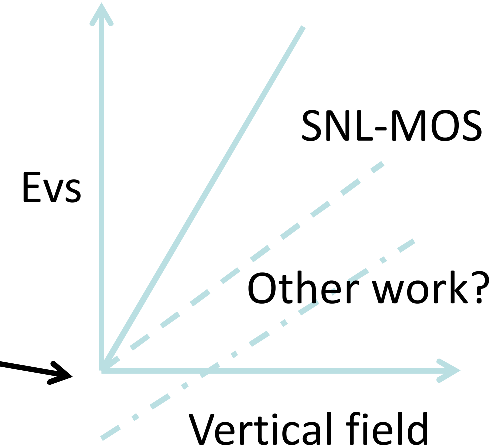

Gamble et al. in preparation

Characterization of tunnel barriers

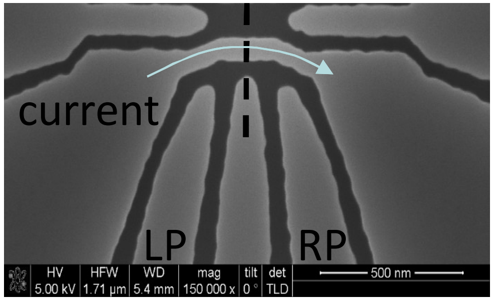

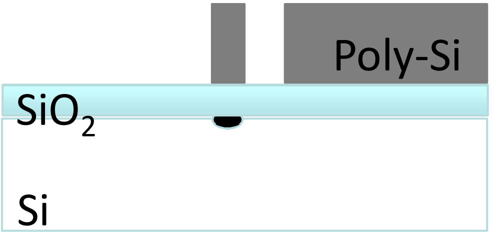

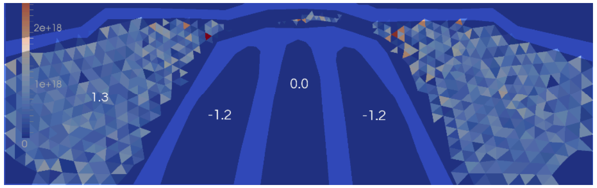

- Central component of quantum dots is the tunnel barrier
- Challenge: complex dependences on geometry and voltages [Friesen et al., …] – hard to model
- Crude first approach:
  - Use simplified parameteric model that captures barrier height, width, V dependence
  - Find measurement method that can produce rapid characterization
  - Begin to calibrate models

Characterization of tunnel barriers

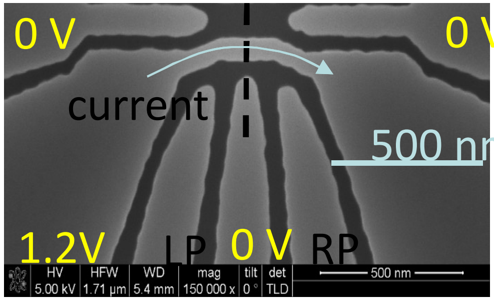

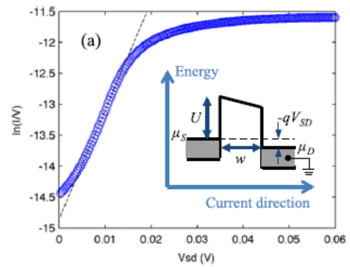

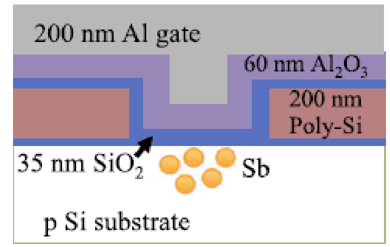

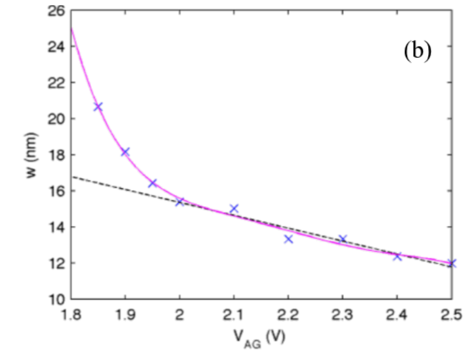

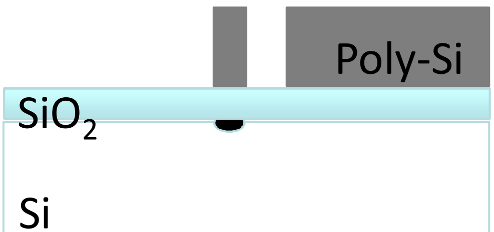

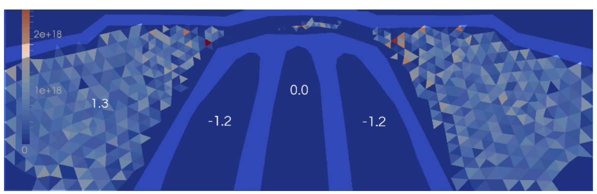

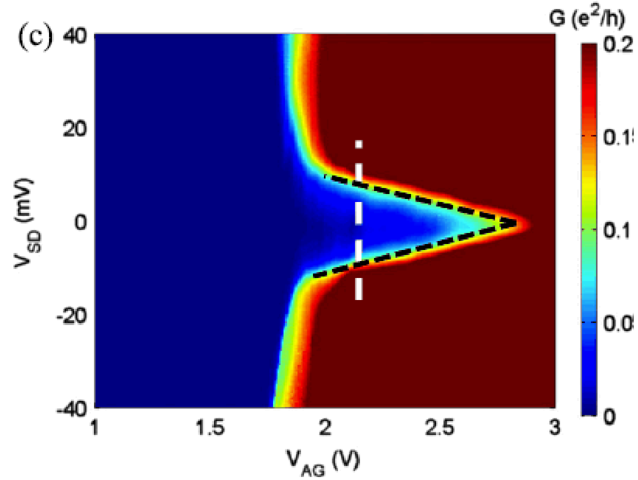

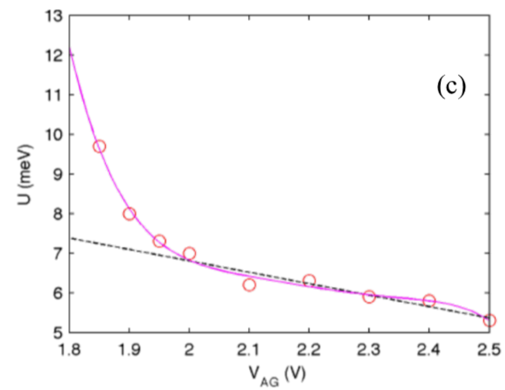

- Central component of quantum dots is the tunnel barrier
- Challenge: complex dependences on geometry and voltages [Friesen et al., …] – hard to model
- Crude first approach:
  - Use simplified parameteric model that captures barrier height, width, V dependence
  - Find measurement method that can produce rapid characterization
  - Begin to calibrate models

Shirkhorshidian et al. Nanotechnology 26 (2015)

Poly silicon quantum dot

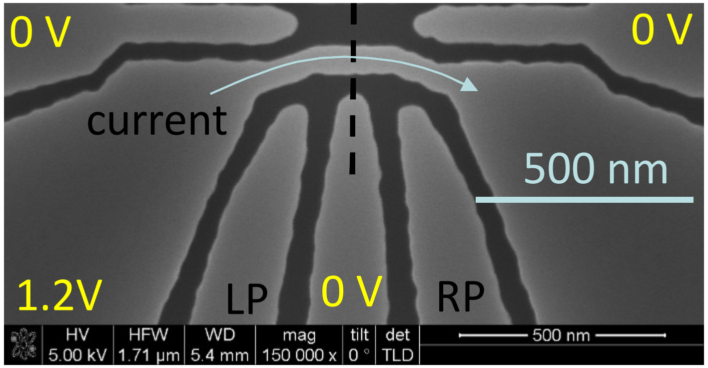

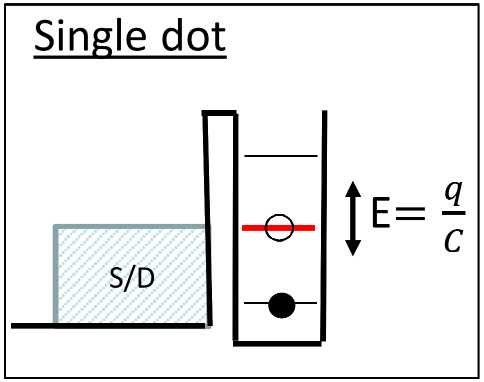

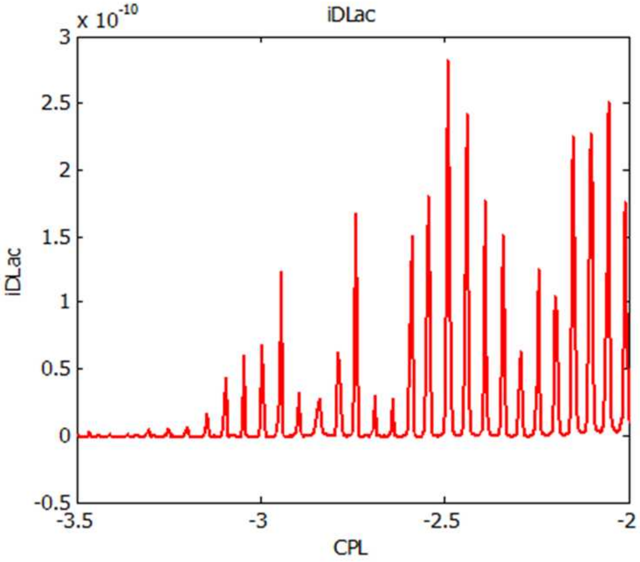

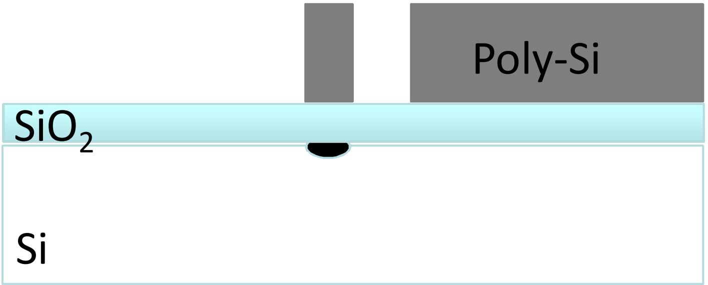

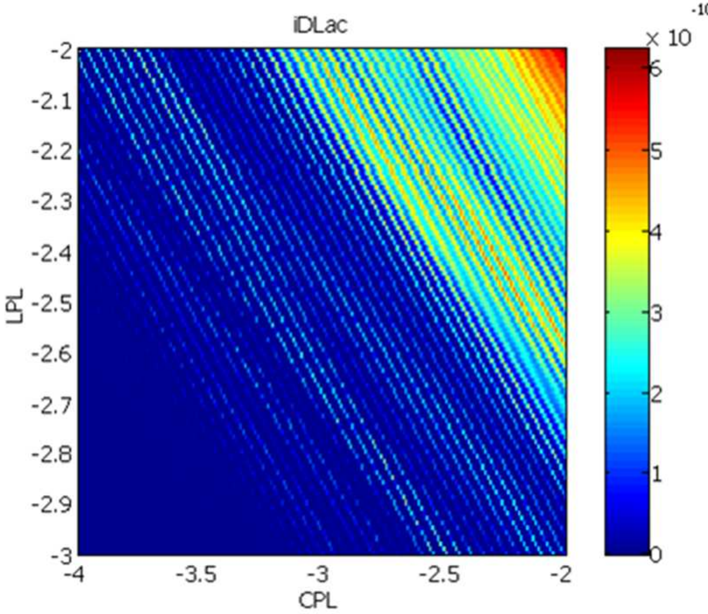

- Relatively regular period Coulomb blockade achieved in poly silicon SET
- Wire width ~50-70 nm with gaps between wire and plunger of ~40-50 nm at tips
- Disorder in potential is still observed in effects on non-linear modulation of tunnel barriers
  - Modulation of conductance not monotonic

Magnetospectroscopy

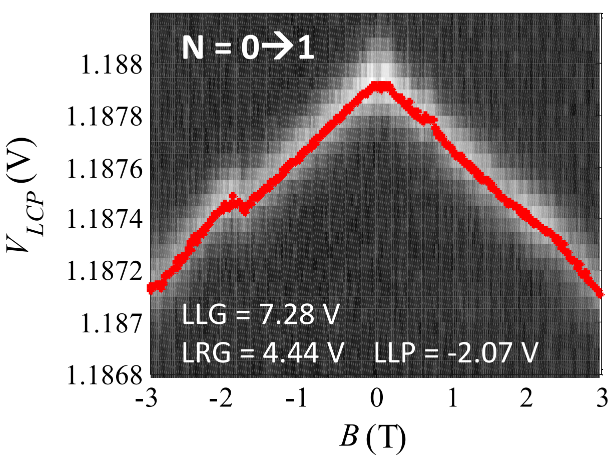

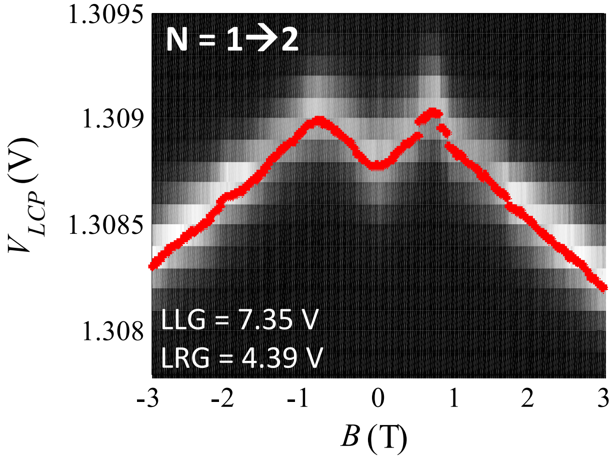

- Stable – allows reasonably sharp magnetospectroscopy
- Single spin filling for N=1
- Singlet triplet splitting of 1T for N=2
    - Assume lowest lying ES is a valley state → valley splitting is 110 ueV
- Valley splitting appears tunable through vertical field (in other measurements)

Charge sensing and finding donors at N=1

- Good charge sense signal from opposing QD
- From experience with gated wires, donors are only visible when the smallest possible lateral field is present
- Retuned SWAG and identified likely donor offsets
- High contrast anti-crossings & indications of tunable tunnel coupling

C_{gate}/C_{LLP}	LCP	LLP	LRP
QD-9	6.67	1.00	0.89
D-B	1.93	1.00	0.18
D-C	4.39	1.00	1.03

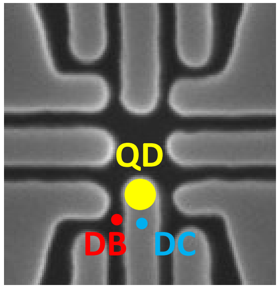

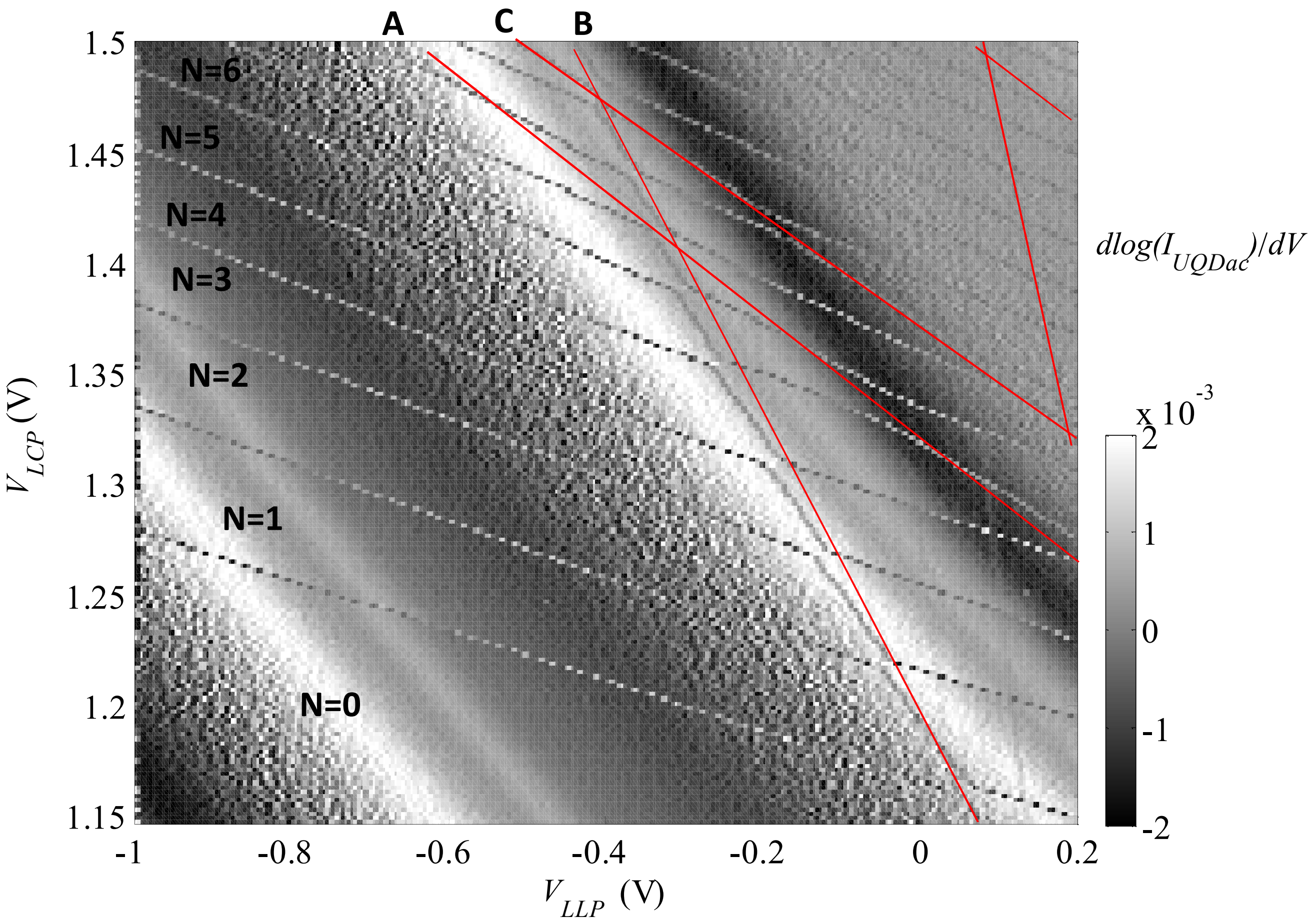

Higher contrast charge transition

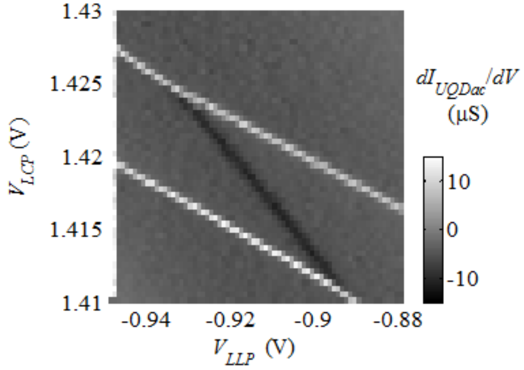

Rudolph
Sandia National Laboratories

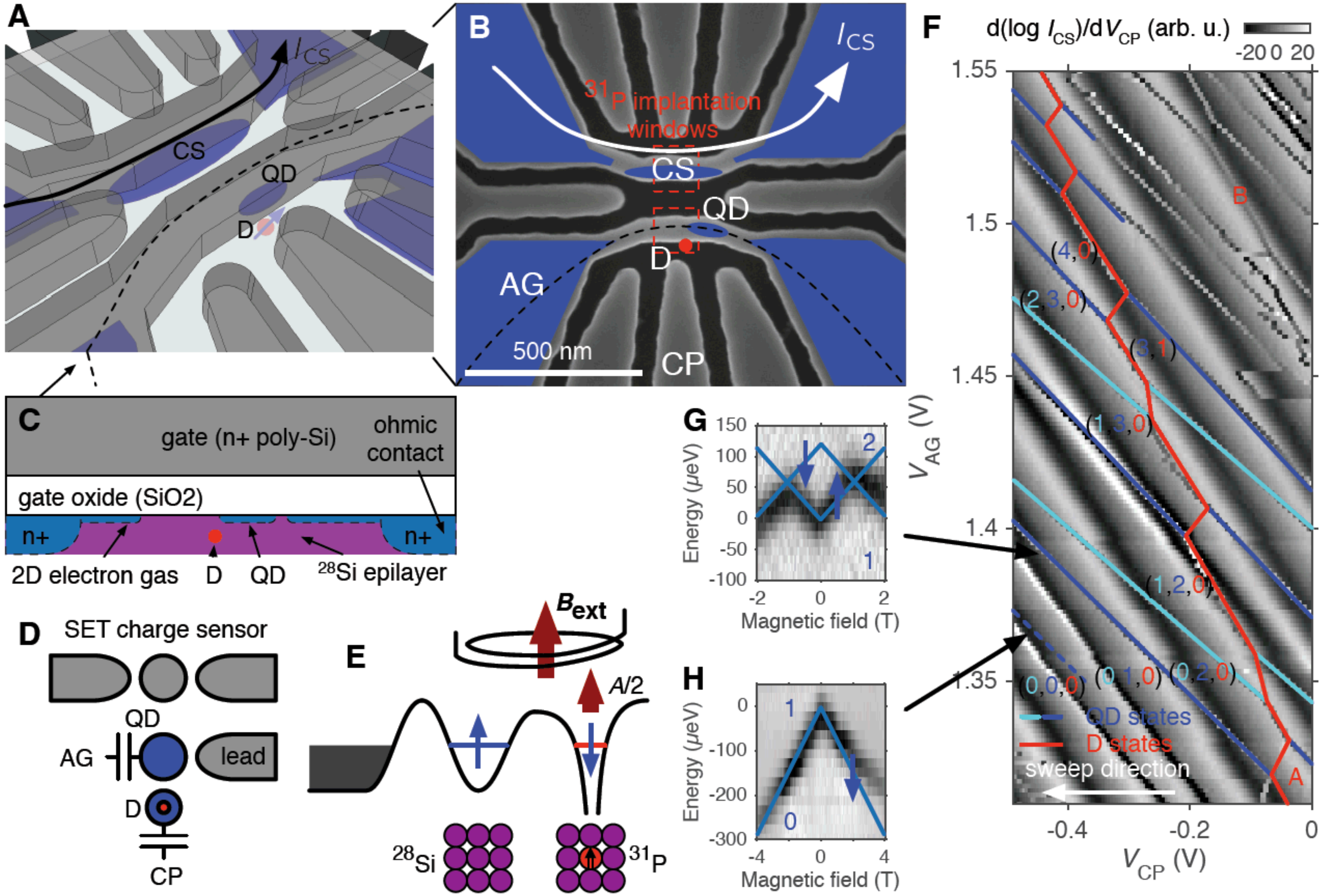

A
I_{CS}
CS
QD
D
B
I_{CS}
^{31}P implantation windows
CS
QD
D
AG
500 nm
CP
C
gate (n+ poly-Si)
ohmic contact
gate oxide (SiO2)
n+
n+
2D electron gas
D
QD
^{28}Si epilayer
D
SET charge sensor
QD
AG
lead
D
CP
E
B_{ext}
$A/2$
^{28}Si
^{31}P
F
d(log I_{CS})/dV_{CP} (arb. u.)
-20 0 20
1.55
1.5
1.45
1.4
1.35
V_{AG} (V)
-0.4
-0.2
0
V_{CP} (V)
B
(4,0)
(2,3,0)
(3,1)
(1,3,0)
(1,2,0)
(0,0,0)
(0,1,0)
(0,2,0)
QD states
D states
sweep direction
A
G
Energy (μeV)
150
100
50
0
-50
-100
-2
0
2
Magnetic field (T)
2
1
H
Energy (μeV)
0
-100
-200
-300
-4
0
4
Magnetic field (T)
1
0

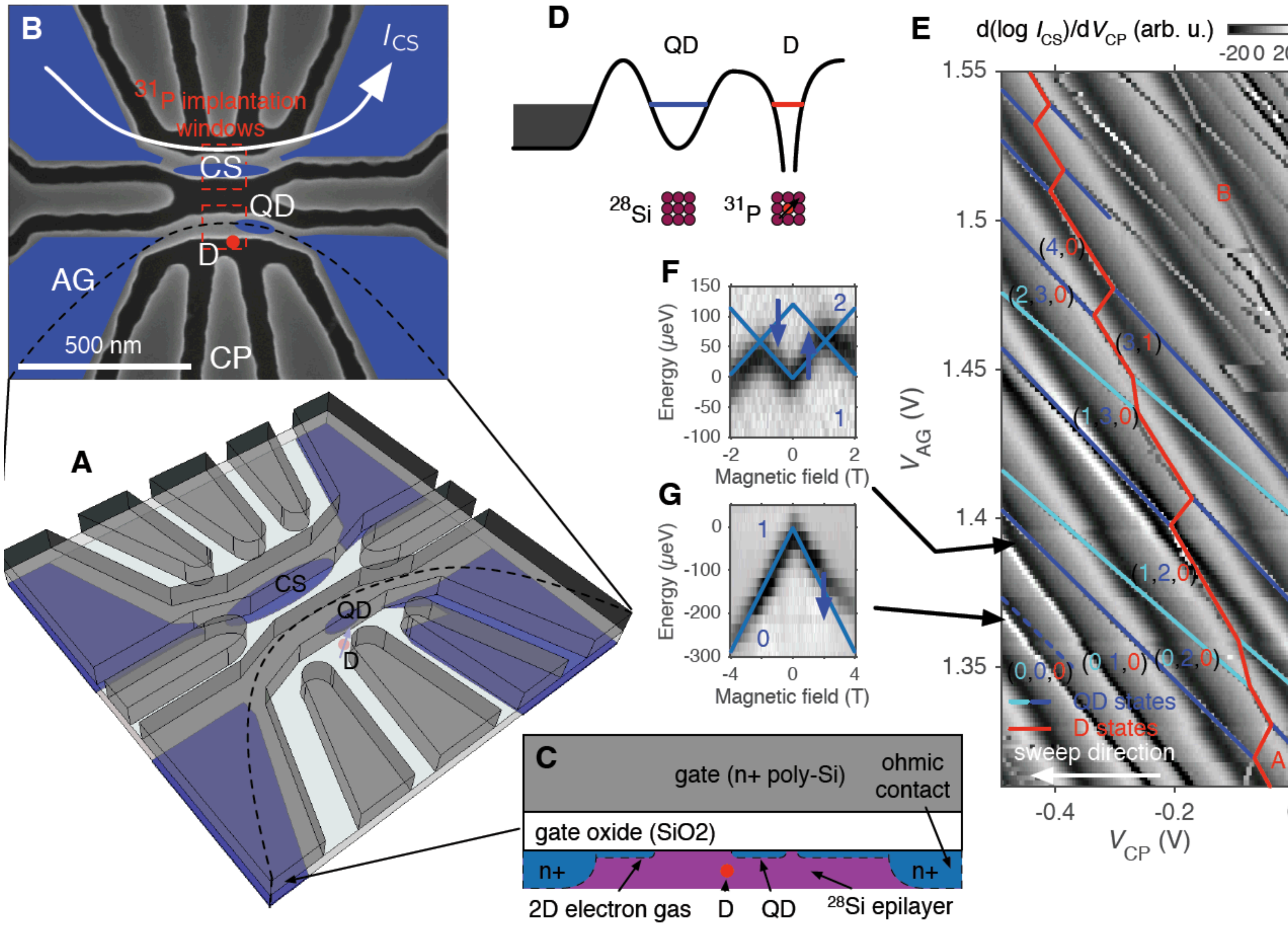

B
I_{CS}
31P implantation windows
CS
QD
D
AG
500 nm
CP
A
CS
QD
D
D
QD
D
28Si
31P
E
d(log I_{CS})/dV_{CP} (arb. u.)
-20 0 20
1.55
1.5
1.45
1.4
1.35
V_{AG} (V)
B
(4,0)
(2,3,0)
(3,1)
(1,3,0)
(1,2,0)
(0,0,0)
(0,1,0)
(0,2,0)
QD states
D states
sweep direction
A
-0.4
-0.2
0
V_{CP} (V)
F
Energy (μeV)
150
100
50
0
-50
-100
-2
0
2
Magnetic field (T)
G
Energy (μeV)
0
-100
-200
-300
-4
0
4
Magnetic field (T)
C
gate (n+ poly-Si)
ohmic contact
gate oxide (SiO2)
n+
n+
2D electron gas
D
QD
28Si epilayer

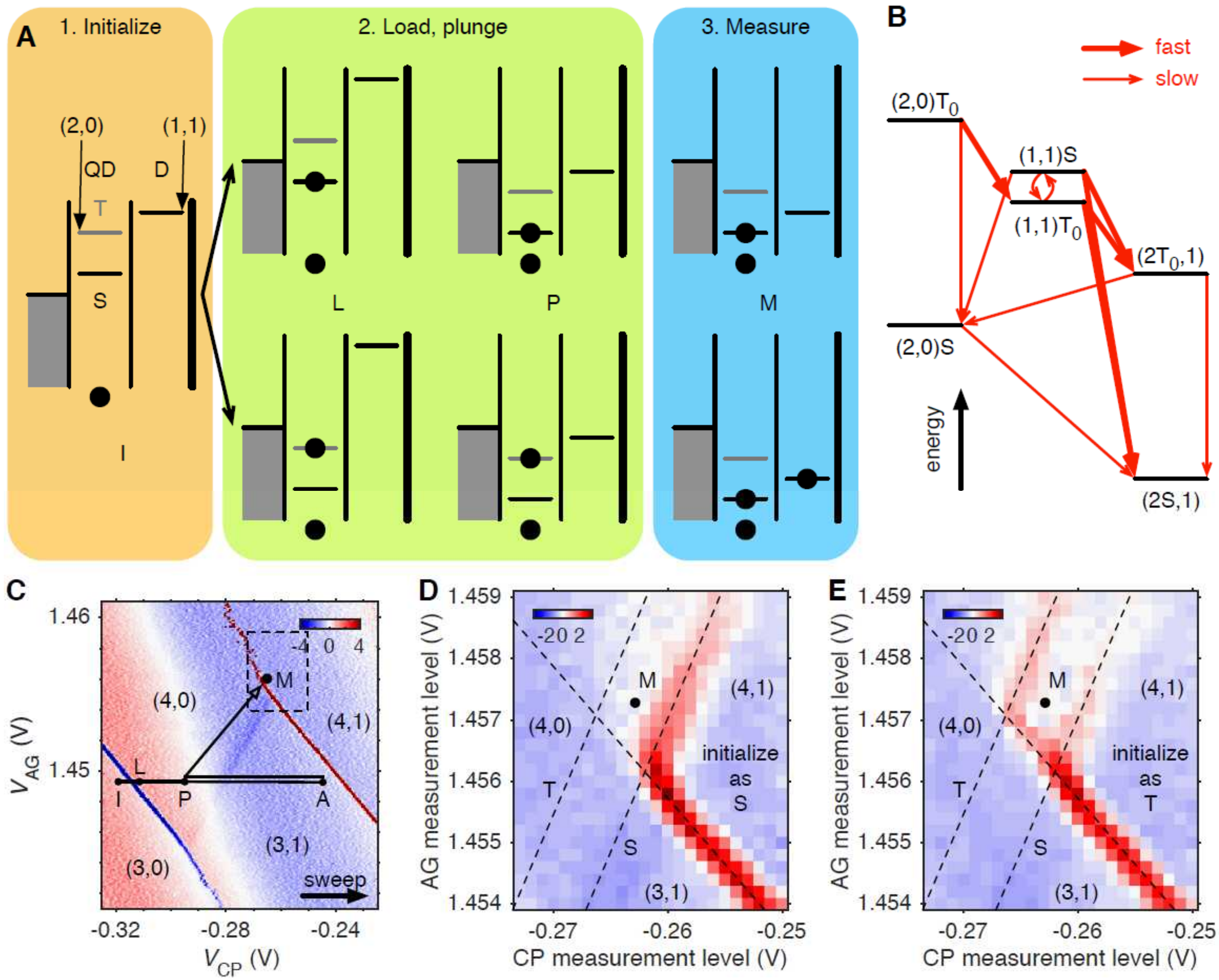

A
1. Initialize
(2,0)
(1,1)
QD
D
T
S
I
2. Load, plunge
L
P
3. Measure
M
B
fast
slow
(2,0)T0
(1,1)S
(1,1)T0
(2T0,1)
(2,0)S
(2S,1)
energy
C
1.46
1.45
VAG (V)
(4,0)
(4,1)
(3,0)
(3,1)
M
L
I
P
A
sweep
-4 0 4
-0.32
-0.28
-0.24
VCP (V)
D
1.459
1.458
1.457
1.456
1.455
1.454
AG measurement level (V)
-20 2
M
(4,0)
(4,1)
initialize as S
T
S
(3,1)
-0.27
-0.26
-0.25
CP measurement level (V)
E
1.459
1.458
1.457
1.456
1.455
1.454
AG measurement level (V)
-20 2
M
(4,0)
(4,1)
initialize as T
T
S
(3,1)
-0.27
-0.26
-0.25
CP measurement level (V)

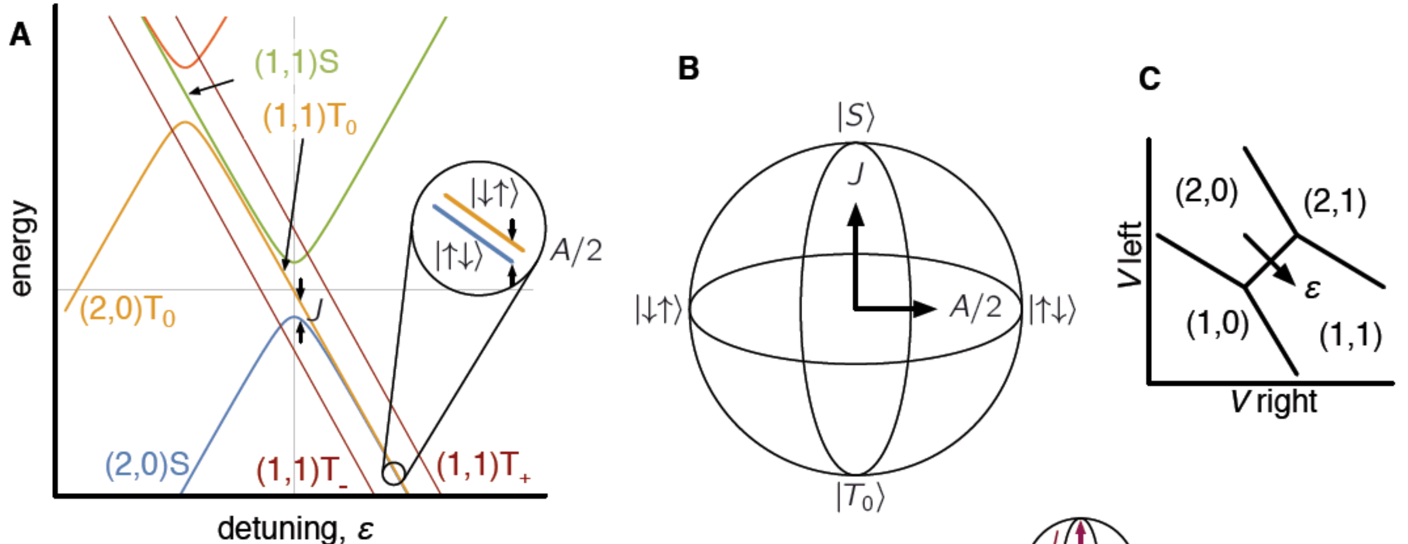
A
energy
detuning, ε
(1,1)S
(1,1)T0
(2,0)T0
J
|↓↑⟩
|↑↓⟩
A/2
(2,0)S
(1,1)T-
(1,1)T+
B
|S⟩
J
|↓↑⟩
A/2
|↑↓⟩
|T0⟩
C
(2,0)
(2,1)
V left
ε
(1,0)
(1,1)
V right

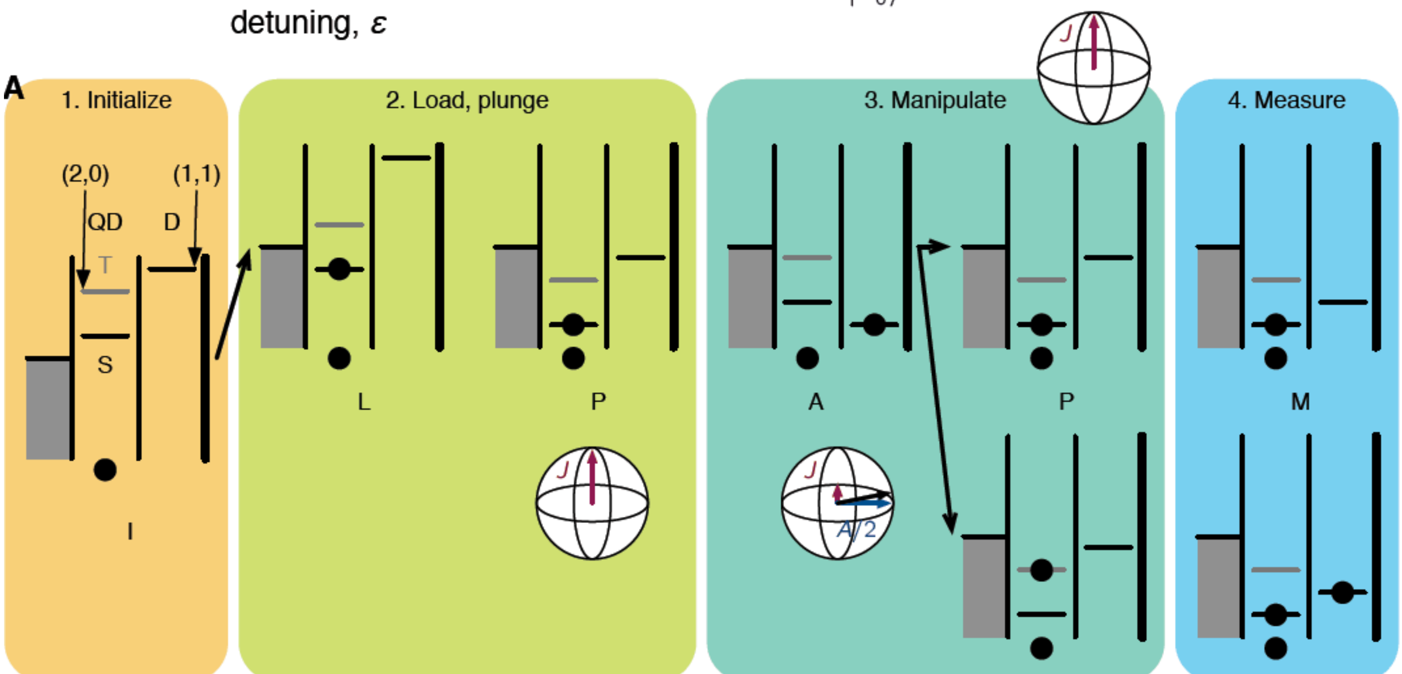
A
1. Initialize
(2,0)
(1,1)
QD
D
T
S
I
2. Load, plunge
L
P
J
3. Manipulate
J
A
P
J
A/2
4. Measure
M

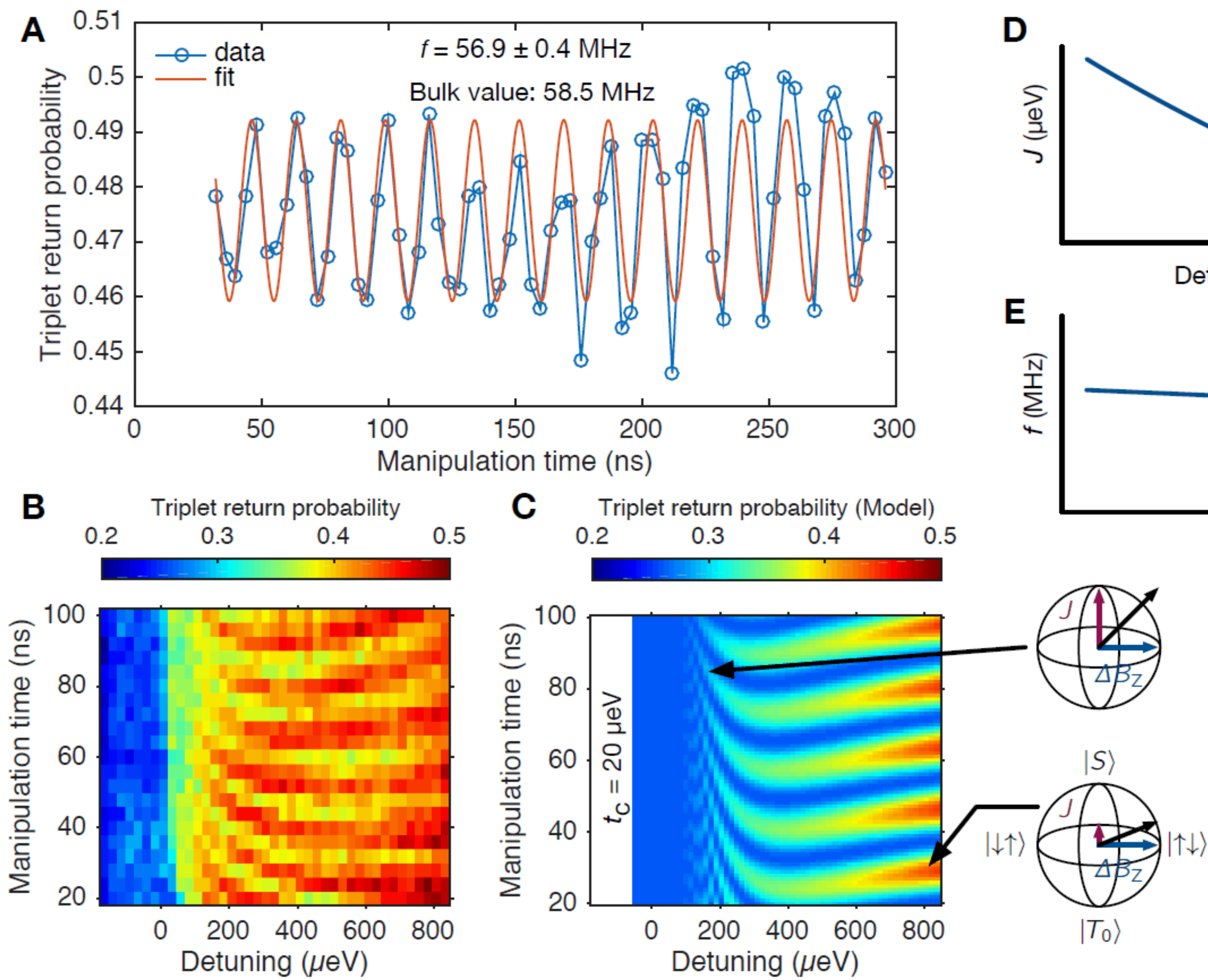
A
data
fit
$f = 56.9 \pm 0.4$ MHz
Bulk value: 58.5 MHz
Triplet return probability
Manipulation time (ns)
B
Triplet return probability
Manipulation time (ns)
Detuning (μeV)
C
Triplet return probability (Model)
$t_C = 20$ μeV
Manipulation time (ns)
Detuning (μeV)
D
J (μeV)
Detuning (μeV)
E
f (MHz)
time (h)
J
ΔB_Z
|S⟩
|↓↑⟩
|↑↓⟩
$|T_0\rangle$